(2)

NRL Memorandum Report 5607

AD-A157 534

Total and Partial Absorption Coefficients for a Nitrogen Plasma

R. D. TAYLOR

Berkeley Research Associates
Springfield, VA 22150

A. W. ALI

Plasma Physics Division

July 2, 1985

This report was supported by the Defense Advanced Research Projects Agency (DoD), ARPA Order No. 4395, Amendment 54, monitored by the Naval Surface Weapons Center under Contract No. N60921-85-WR-W0131.

NAVAL RESEARCH LABORATORY
Washington, D.C.

ADA 157 534

SECURITY CLASSIFICATION OF THIS PAGE

REPORT DOCUMENTATION PAGE

1a. REPORT SECURITY CLASSIFICATION: UNCLASSIFIED	1b. RESTRICTIVE MARKINGS
2a. SECURITY CLASSIFICATION AUTHORITY	3. DISTRIBUTION/AVAILABILITY OF REPORT: Approved for public release; distribution unlimited.
2b. DECLASSIFICATION/DOWNGRADING SCHEDULE	
4. PERFORMING ORGANIZATION REPORT NUMBER(S): NRL Memorandum Report 5607	5. MONITORING ORGANIZATION REPORT NUMBER(S)
6a. NAME OF PERFORMING ORGANIZATION: Naval Research Laboratory; 6b. OFFICE SYMBOL (If applicable): Code 4700.1	7a. NAME OF MONITORING ORGANIZATION: Naval Surface Weapons Center
6c. ADDRESS (City, State, and ZIP Code): Washington, DC 20375-5000	7b. ADDRESS (City, State, and ZIP Code): White Oak, Silver Spring, MD 20910
8a. NAME OF FUNDING/SPONSORING ORGANIZATION: DARPA; 8b. OFFICE SYMBOL (If applicable)	9. PROCUREMENT INSTRUMENT IDENTIFICATION NUMBER: ARPA Ord. - 4395
8c. ADDRESS (City, State, and ZIP Code): Arlington, VA 22209	10. SOURCE OF FUNDING NUMBERS: PROGRAM ELEMENT NO. 62707E; PROJECT NO.; TASK NO.; WORK UNIT ACCESSION NO. DN680-415

11. TITLE (Include Security Classification)
Total and Partial Absorption Coefficients for a Nitrogen Plasma

12. PERSONAL AUTHOR(S)
Taylor, R.D.* and Ali, A.W.

13a. TYPE OF REPORT	13b. TIME COVERED	14. DATE OF REPORT (Year, Month, Day)	15. PAGE COUNT
Interim	FROM 1984 TO 1985	1985 July 2	53

16. SUPPLEMENTARY NOTATION
*Berkeley Research Associates, Springfield, VA 22150 (Continues)

17. COSATI CODES			18. SUBJECT TERMS (Continue on reverse if necessary and identify by block number)
FIELD	GROUP	SUB-GROUP	Radiative transfer; Absorption coefficient; Absorption cross section; Nitrogen plasma

19. ABSTRACT (Continue on reverse if necessary and identify by block number)

A detailed description of the absorption cross sections in a nitrogen plasma is given. The results are presented for partial and total absorption coefficients, where the components are the bound-bound, the bound free and the free-free absorptions. Use is made of nitrogen plasma composition as a function of the electron density and temperature calculated earlier. Keywords include Radiative Transfer,

20. DISTRIBUTION/AVAILABILITY OF ABSTRACT: ☒ UNCLASSIFIED/UNLIMITED ☐ SAME AS RPT. ☐ DTIC USERS	21. ABSTRACT SECURITY CLASSIFICATION: UNCLASSIFIED
22a. NAME OF RESPONSIBLE INDIVIDUAL: A. W. Ali	22b. TELEPHONE (Include Area Code): (202) 767-3762; 22c. OFFICE SYMBOL: Code 4700.1

DD FORM 1473, 84 MAR — 83 APR edition may be used until exhausted. All other editions are obsolete.

SECURITY CLASSIFICATION OF THIS PAGE

16. SUPPLEMENTARY NOTATION (Continued)

This report was supported by the Defense Advanced Research Projects Agency (DoD), ARPA Order No. 4395, Amendment 54, monitored by the Naval Surface Weapons Center under Contract No. N60921-85-WR-W0131.

CONTENTS

TOTAL AND PARTIAL ABSORPTION COEFFICIENTS FOR A NITROGEN PLASMA

I. INTRODUCTION

When an intense electron beam is propagated through the atmosphere a hot, ionized channel is created. A detailed picture of the chemistry and physics within the channel is crucial to the understanding and modeling of electron beam propagation through the atmosphere.

An issue of current importance is channel cooling, specifically, to what extent does energy relax from the heated channel to the surrounding environment. To determine the role of radiation emission and transport through the channel, one must perform a detailed radiative transfer calculation. The primary ingredient for such a calculation is the absorption coefficient. For electron temperatures of ~3 e.v., for example, nitrogen and oxygen atoms and their ions are the dominant constituents of heated air. In this paper we present the atomic absorption coefficients for a nitrogen plasma using a model reported earlier [1]. The relevant photoabsorption and photoionization cross sections are also given.

Johnston et. al. [3] have studied the radiative properties of high temperature air in detail. Their calculations assume an equilibrium composition for air of varying densities and include thousands of line and photoionization transitions. While the emphasis of their

Manuscript approved May 3, 1985.

work is for temperatures less than 1 e.v., and thus on accurately describing the molecular absorption coefficient, they extend the calculations to much higher temperatures where the atomic component is dominant. It is in this regime that we compare results.

II. ABSORPTION AND IONIZATION CROSS SECTIONS

Specific details of our model for the nitrogen plasma may be found elsewhere [1]. For electron temperatures of 1-3 e.v. we assume the plasma consists of N, N^+, N^{++}, and electrons and include in our calculation the lowest thirteen (13) levels of N I, the lowest seventeen (17) levels of N II, and two representative levels for N III. This simple model for nitrogen includes the dominant uv and visible emissions arising from bound-bound and free-bound transitions. In this section the absorption cross sections for all bound-bound, bound-free, and free-free transitions contained within our model are described in detail.

A. Bound-Bound Transitions

The photoabsorption cross section for transitions between a lower level ℓ and an upper level u is given [2] by,

$$\sigma_{\nu u \ell} = \sigma_{\nu u \ell, m} \frac{(\Delta\nu)^2}{(\nu - \nu_{u\ell})^2 + (\Delta\nu)^2} \tag{1}$$

where

$$\sigma_{\nu u \ell, m} = \frac{\lambda^2}{8\pi^2} \frac{g_u}{g_\ell} \frac{A_{u\ell}}{\Delta\nu} \tag{2}$$

Equations (1) and (2) assume a Lorentzian line shape for the transition whose resonance frequency is $\nu_{u\ell}$ and wavelength is λ. The statistical weights of the upper and lower states are g_u and g_ℓ, $A_{u\ell}$ is the Einstein coefficient, and $\Delta\nu$ the line width. Contributions to line broadening include Stark and Doppler broadening. We calculate the contribution of each as a function of frequency, electron temperature, and electron density and choose $\Delta\nu$ to be the greater of the two. For example, at high temperatures and low electron densities, the Doppler width is greatest whereas larger electron densities cause the Stark effect to dominate. The Stark width is always larger for electron densites greater than $10^{18}/cm^3$. The necessary Stark widths were obtained from reference [4], either directly or through an interpolation procedure for those transitions included in our model but not listed in Griem's tables.

We recognize that in situations where there are two broadening mechanisms, one resulting in a Gaussian line shape and the other in a Lorentzian line shape, the proper description involves Voigt profiles with an appropriately defined width. However, the above model has been chosen for simplicity and is not expected to significantly alter the results.

Figures (1a) - (3a) show the bound-bound absorption cross sections for electron temperatures of 1.0, 2.0, and 3.0 e.v.. Details of the plasma composition (Ne, N, N^+, N^{++}) are discussed in section III. For all three cases the lines are Stark broadened at all photon energies. As the electron temperature increases and the plasma contains more electrons the lines broaden with a corresponding decrease in the absorption maximum. At Te = 1.0 e.v. the cross sections peak at approximately 10^{-14} - 10^{-13} cm^2. For higher temperatures there is a drop of nearly two orders of magnitude.

B. Bound-Free Transitions

The photoionization cross sections have been obtained from several sources. The following functional form was introduced by Henry [5] and used by Ali [6] to describe photoionization from the ground state configurations of N,

$$\sigma_\lambda = \sigma_{th} [\alpha(\lambda/\lambda_0)^s + (1-\alpha)(\lambda/\lambda_0)^{s+1}] \times 10^{-18} \text{ cm}^2 \quad (3)$$

The parameters α, s , and σ_{th} can be found in reference [6b]. In our calculations, the threshold wavelengths λ_0 have been corrected for the reduction in ionization potential due to the immersion of an isolated atom in a plasma in the manner described in reference [1].

The quantum-defect method [7] provides a good approximation to nonhydrogenic continuous absorption cross sections. Griem [7] has tabulated these cross sections for various atoms including neutral nitrogen. For bound-free transitions between $N^{z-1}(n,\ell)$ and N^{z}, where n and ℓ are the principal and angular momentum quantum numbers of the initial atomic or ionic bound state, the cross section is given by

$$\sigma_{n\ell}^{z-1} = 15.8\times10^{-18}\,\frac{g^{z}}{g_{n\ell}}\,\frac{n^{3}}{z^{2}}\,\frac{\nu_{n}^{3}}{\nu^{3}}\,f_{n\ell}(\nu) \qquad (4)$$

Here, $g_{n\ell}$ is the statistical weight of the initial state, g^{z} the statistical weight of the final state, ν the frequency of the photon, and ν_n the threshold transition frequency (again corrected for the ionization potential reduction). For neutral nitrogen, the frequency-dependent factor $f_{n\ell}(\nu)$, is computed using a linear interpolation procedure based on the information provided in reference [7]. For N^{+}, an average value of 0.2 is used.

The results are shown in Figs. (1b) - (3b). Structurally, the cross sections are similiar. Bound-free absorption is important for visible and uv frequencies. The onset of different absorptions depend on the threshold frequency; this in turn depends on the electron density and temperature through the the ionization potential reduction. The cross section varies between 10^{-17} and 10^{-16} cm^2, and is a small contribution compared to bound-bound absorption in the visible regime, but is a significant contribution in the uv regime.

C. Free-Free Transitions

Free-free transitions occur when a photon is absorbed by an electron moving in the field of an ion or neutral, thereby increasing the energy of the electron. For the case of inverse Bremsstrahlung involving ions Kramer's formula modified by a Gaunt factor [8] provides a good estimate for the "cross section". Specifically, we use

$$\sigma_{ff}^{+} = 2.43\times10^{-37} \frac{z^2}{Te^{1/2}} \frac{\langle g_{ff}\rangle}{(h\nu)^3} \qquad \frac{cm^5}{\text{ion-elect.}} \qquad (5)$$

where z is the net charge on the ion, Te the temperature in e.v., $h\nu$ the photon energy in e.v., and $\langle g_{ff}\rangle$ the Gaunt factor averaged over a Maxwellian electron velocity distribution. In the field of N^+ this factor varies with temperature between 1.29 and 1.36; we have chosen an average value of 1.325. In the presence of N^{++} it varies between 1.175 and 1.26; here we use $\langle g_{ff}\rangle = 1.225$.

Free-free transitions in the fields of the neutrals are accounted for by the formula of Mjolsness and Ruppel [9]. This simple approximation, also used by Johnston et al. [3], is

$$\sigma_{ff}^{0} = 2.20\times10^{-39}\ Te^{3/2}\ \frac{\sigma_0}{(h\nu)^3}\left(1 + \frac{h\nu}{2Te}\right)\ \frac{cm^5}{\text{neu.-elect.}} \tag{6}$$

where σ_0 = .80 for N. Geltman [10] has tabulated the absorption coefficients and cross sections for free-free radiation in electron-neutral collisions for different atomic species over a temperature range of 500 - 20000 °K and wavelengths between .5 and 20 μm. Eq. (6) gives results which differ from his by a factor of 2 at most.

For comparison with bound-bound and bound-free cross sections, eqs. (5) and (6) must be multiplied by Ne. On a log-log scale, both show essentially linearly decreasing behavior with increasing photon energy over the range of interest. The neutral cross section is two orders of magnitude less than that due to N^+. At low temperatures the free-free cross sections are negligible compared to the others. However, at high temperatures and low photon energies they are of the same magnitude as the bound-free cross sections. As shown in section III these processes contribute significantly to the total absorption coefficient.

Finally, the total cross sections are shown in Figs. (1c) - (3c). Their behavior reflects the above discussion.

III. ATOMIC ABSORPTION COEFFICIENTS

The absorption coefficient, corrected for stimulated emission and defined as a function of photon frequency, is generally partitioned according to the various contributing processes, i.e.

$$\kappa_\nu = \kappa_{bb} + \kappa_{bf} + \kappa_{ff}^0 + \kappa_{ff}^+ \quad (\mathrm{cm}^{-1}) \tag{7}$$

where the individual bound-bound, bound-free, and free-free coefficients are given by

$$\kappa_{bb} = \sum_{z,\ell} N_\ell^{z-1} \sum_u \sigma_{u\ell}^{z-1} \tag{8}$$

$$\kappa_{bf} = \sum_{z,\ell} N_\ell^{z-1} \sum_u \sigma_{u\ell}^{z-1} \tag{9}$$

$$\kappa_{ff}^0 = N\ Ne\ \sigma_{ff}^0 \tag{10}$$

$$\kappa_{ff}^+ = N^+\ Ne\ \sigma_{ff}^+ \tag{11}$$

In equations (8) - (11) N_ℓ^{z-1}, Ne, N, and N^+ are the population density for nitrogen in state ℓ and ionization stage z-1, the total electron density, the total neutral density, and the total N^+ density, respectively. The cross sections are those discussed in the previous section. In eq. (8), u denotes the final state of the atom or ion in the same ionization stage after absorption, while in eq. (9) it denotes the state of the ion in the next higher ionization stage.

A. Plasma Composition

The detailed calculation of the absorption coefficient requires the population densities of all species in all states. In the present calculation we assume an initial neutral nitrogen density comparable to that found in equilibrium air [2,11] at the temperatures of interest. For an initial electron density of 10^{17} /cm^3, the detailed rate equations given in reference [1] are integrated until a steady state is reached. The final populations of all states contained within our model are then used to calculate the absorption coefficients given above. Tables I and II show a comparison between the final N, N^+, N^{++}, and Ne densities for our model plasma (I) and the corresponding contribution to equilibrium air (II); a state-specific decomposition is not shown.

B. Absorption Coefficients

The total absorption coefficients, defined in eq.(7), are shown in Figures (1d) - (3d). Explicit representations of the bound-bound, bound-free, and free-free contributions are also shown specifically, in Figures (1e-1h) - (3e-3h).

At Te = 1.0 e.v. the absorption coefficient shows detailed structure in the ir and near uv regime due to significant contributions from neutral nitrogen bound-bound transitions. The absorption length for the uv bound-bound radiation is approximately 10^{-6} to 10^{-3} cm while the ir radiation has a length of 10^{-2} to 10^{-1} cm. Bound-free transitions contribute predominately in the visible regime; the absorption length here is on the order of 100 cm. At this temperature the contribution of free-free transitions involving neutrals is nearly equal to that involving ions. This is because the number of neutrals exceeds the number of ions by exactly two orders of magnitude. Free-free absorption only plays a noticeable role for low photon energies (ir - visible).

When the electron temperature and density of the plasma is increased, the total number of ions becomes comparable to the number of neutrals (see Table I). Figures (2d) - (2h) show several effects. In the ir regime the absorption coefficient reflects the changes in the bound-bound cross sections, particularly broader line structure. While free-free transitions in the presence of neutrals contributes very little, the increased number of ions and electrons causes free-free transitions in the ion fields to significantly enhance the absorption coefficient in the ir and visible regime. More highly excited N states also contribute to an increase in κ in the visible regime, through bound-free transitions. In the uv regime there is a noticeable increase in N^+ bound-bound contributions. As before, most uv radiation is absorbed through bound-free transitions.

Finally, the results for Te = 3.0 e.v. are shown in Figures (3d) - (3h). Here the plasma consists largely of N^+ and electrons. In the ir and visible range, the absorption coefficient has increased by approximately a factor of two, largely due to free-free absorption. Bound-bound absorption involving neutrals has less of an effect than that involving ions. A decrease in nitrogen atoms in the ground state configurations has resulted in a corresponding decrease in bound-free uv absorption involving these atoms.

As mentioned earlier, Johnston et. al. [3] have calculated the total absorption coefficient in equilibrium air for a series of temperatures. Their calculations include thousands of bound-bound and bound-free transitions for the dominant atomic and molecular species at each temperature. We have compared the results of our simple model calculation to their results for temperatures of 1.5 and 2.0 e.v.. At these temperatures, air consists largely of nitrogen and oxygen atoms and their ions. The nitrogen concentrations are similiar to those in our model (see

Tables I and II). For photon energies between 1.7 and 100.0 e.v., the general agreement is very good. Excluding the detailed line structure, our absorption coefficient is within a factor of 1.1 - 2.0 throughout. Even the detailed line structure is in reasonable agreement for energies between 1.6 and 20.0 e.v.. Certainly their computations should show more bound-bound contributions due to the inclusion of a complete description of oxygen, as well as more nitrogen transitions. The largest discrepancy is in the ir region, energies less than 1.6 e.v., where our calculations show structure in contrast to theirs, although the average coefficient there still agrees within a factor of three.

Table I

Model Plasma Composition ($/cm^3$)*

Te(e.v)	N^{Total}	N	N^+	N^{++}	Ne
1.0	3.56×10^{19}	3.52×10^{19} .99	3.62×10^{17} .01	9.39×10^{8}	3.62×10^{17}
1.5	3.90×10^{19}	3.23×10^{19} .83	6.72×10^{18} .17	2.88×10^{13}	6.72×10^{18}
2.0	3.93×10^{19}	1.89×10^{19} .48	2.03×10^{19} .52	6.65×10^{15}	2.03×10^{19}
2.5	3.92×10^{19}	8.69×10^{18} .22	3.04×10^{19} .77	1.65×10^{17}	3.07×10^{19}
3.0	3.93×10^{19}	3.90×10^{18} .10	3.40×10^{19} .87	1.41×10^{18} .04	3.68×10^{19}

* Bottom entries give fraction of total nitrogen composition

Table II

Equilibrium Air Nitrogen Composition ($/cm^3$)*

Te(e.v.)	N^{Total}	N	N^+	N^{++}	Ne
1.0	3.45×10^{19}	3.40×10^{19} .99	4.50×10^{17} .01	-	5.60×10^{17}
1.5	3.80×10^{19}	3.25×10^{19} .86	5.50×10^{18} .15	-	6.60×10^{18}
2.0	3.84×10^{19}	2.15×10^{19} .56	1.69×10^{19} .44	-	2.00×10^{19}
2.5	3.85×10^{19}	1.05×10^{19} .27	2.08×10^{19} .54	7.20×10^{18} .19	3.10×10^{19}
3.0	3.85×10^{19}	5.00×10^{18} .13	2.15×10^{19} .56	1.20×10^{19} .32	4.30×10^{19}

* Bottom entries give fraction of total nitrogen composition

IV. CONCLUDING REMARKS

The photoabsorption properties of a model nitrogen plasma have been studied for electron temperatures between 1.0 and 3.0 e.v.. Specifically, the relevant absorption cross sections for processes involving bound-bound, bound-free, and free-free transitions have been computed. Finally, the total and partial absorption coefficients (frequency-dependent) have been obtained for a nitrogen plasma whose composition is similiar to that of high temperature, full density, equilibrium air. The results of this benchmark calculation are consistent and in good agreement with the earlier numerical studies of Johnston et. al.. These absorption cross sections and coefficients provide the necessary input for studying radiative transfer in a nitrogen plasma, the next step in our ongoing program.

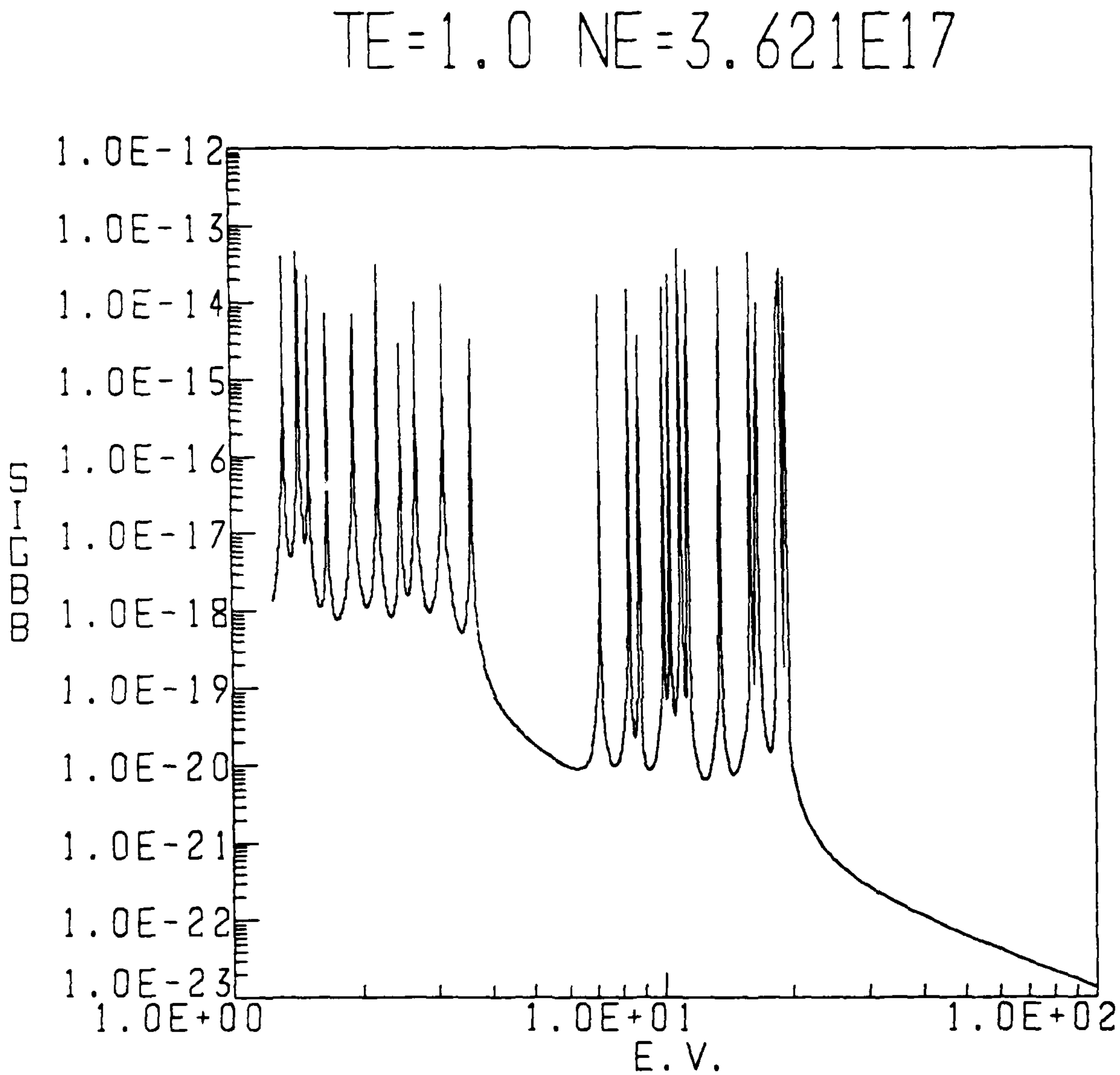

Fig. 1a — Photoabsorption cross section for bound-bound transitions. Te = 1.0 e.v.

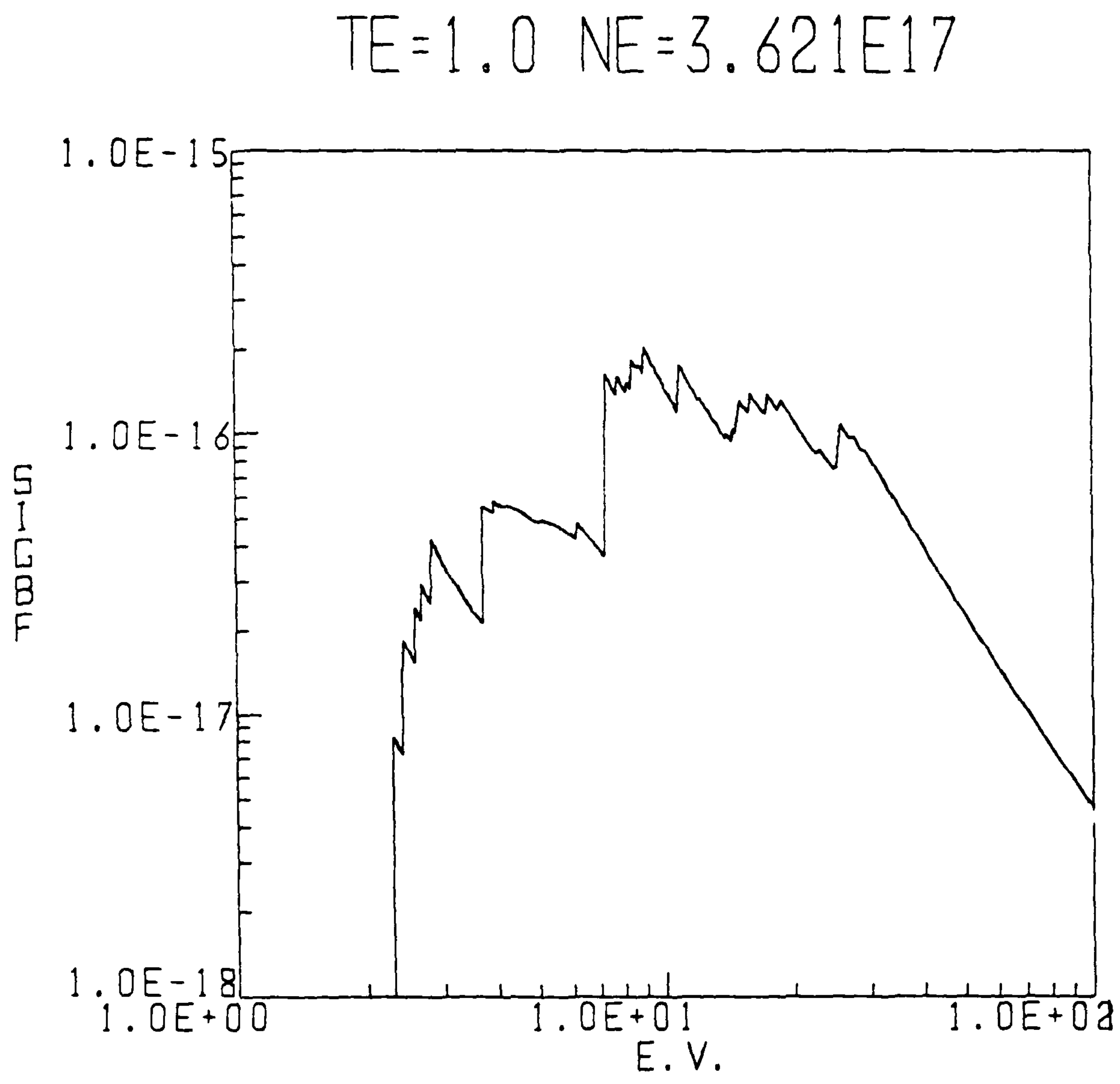

Fig. 1b — Bound-free cross section. Te = 1.0 e.v.

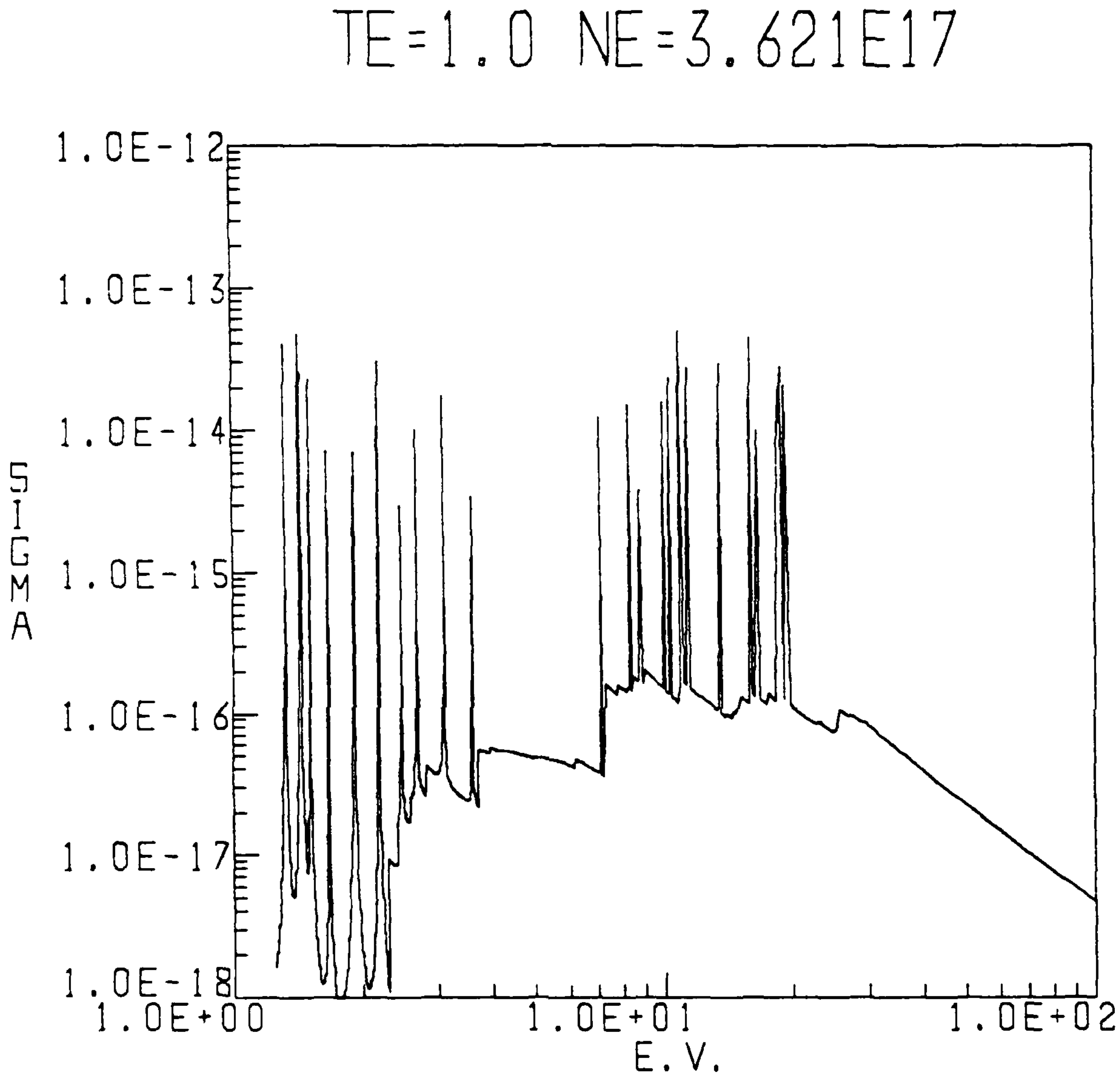

Fig. 1c — Total photoabsorption cross section. Te = 1.0 e.v.

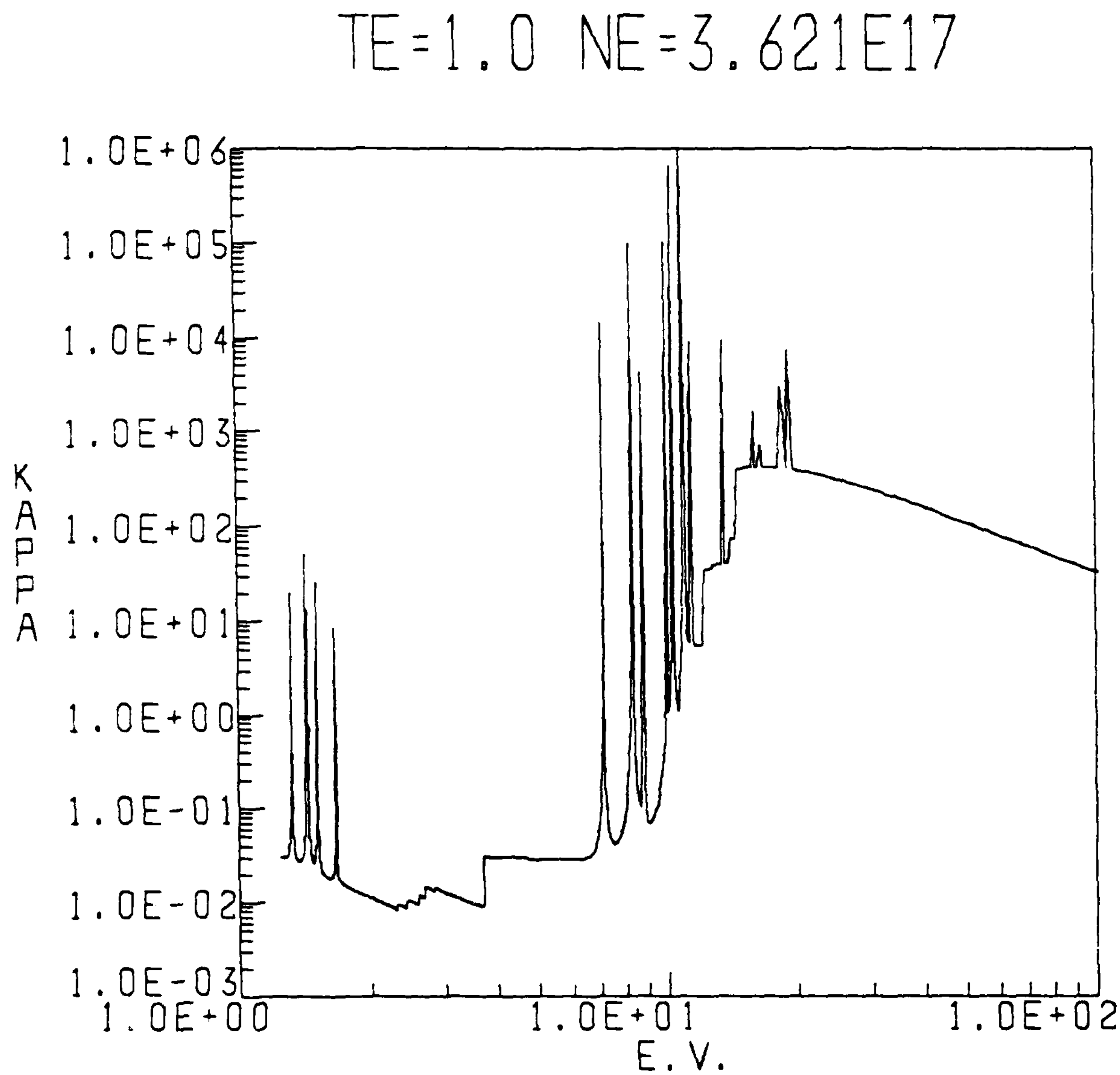

Fig. 1d — Total photoabsorption coefficient. Te = 1.0 e.v.

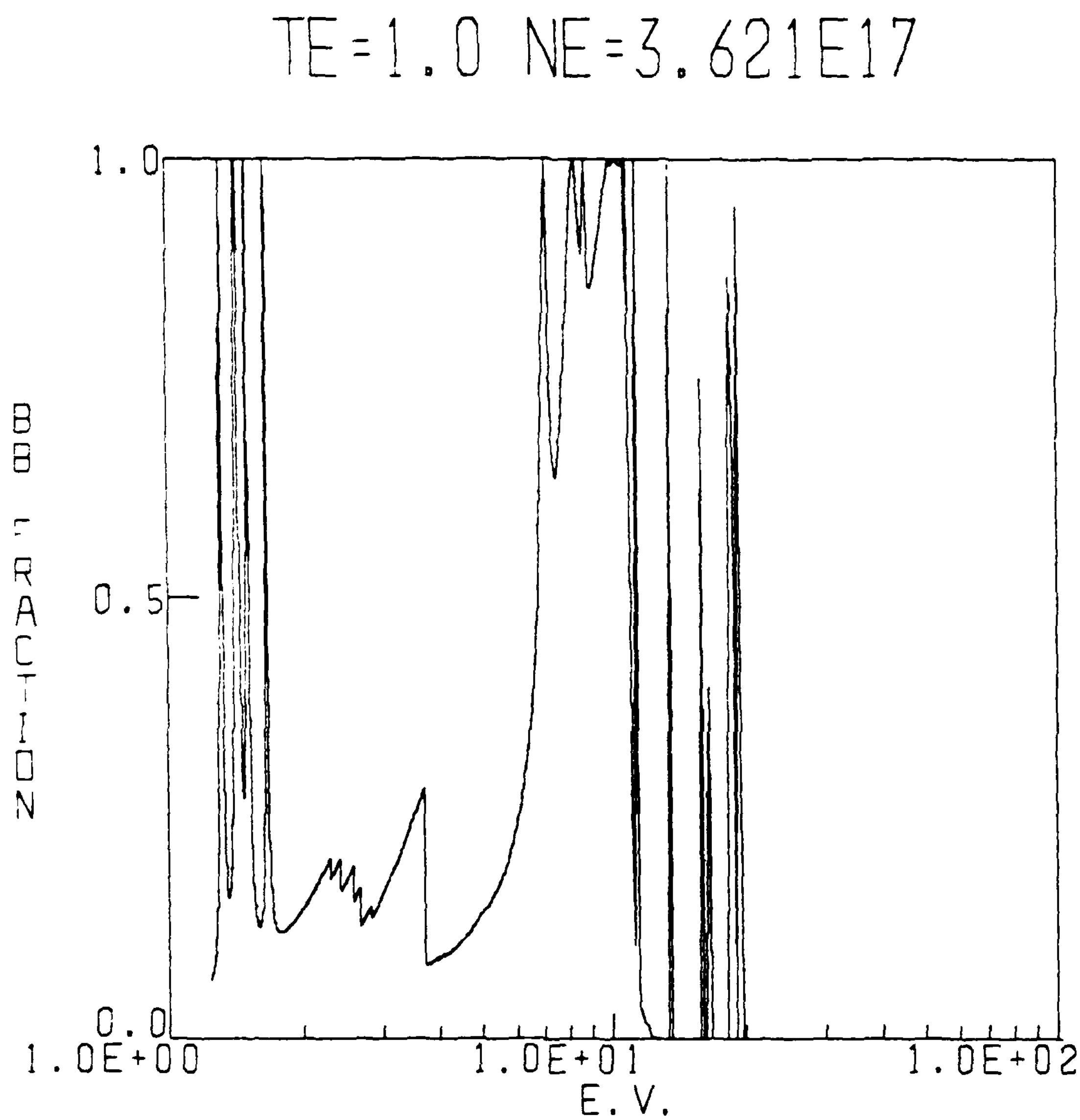

Fig. 1e — Fraction of the total photoabsorption coefficient due to bound-bound transitions. Te = 1.0 e.v.

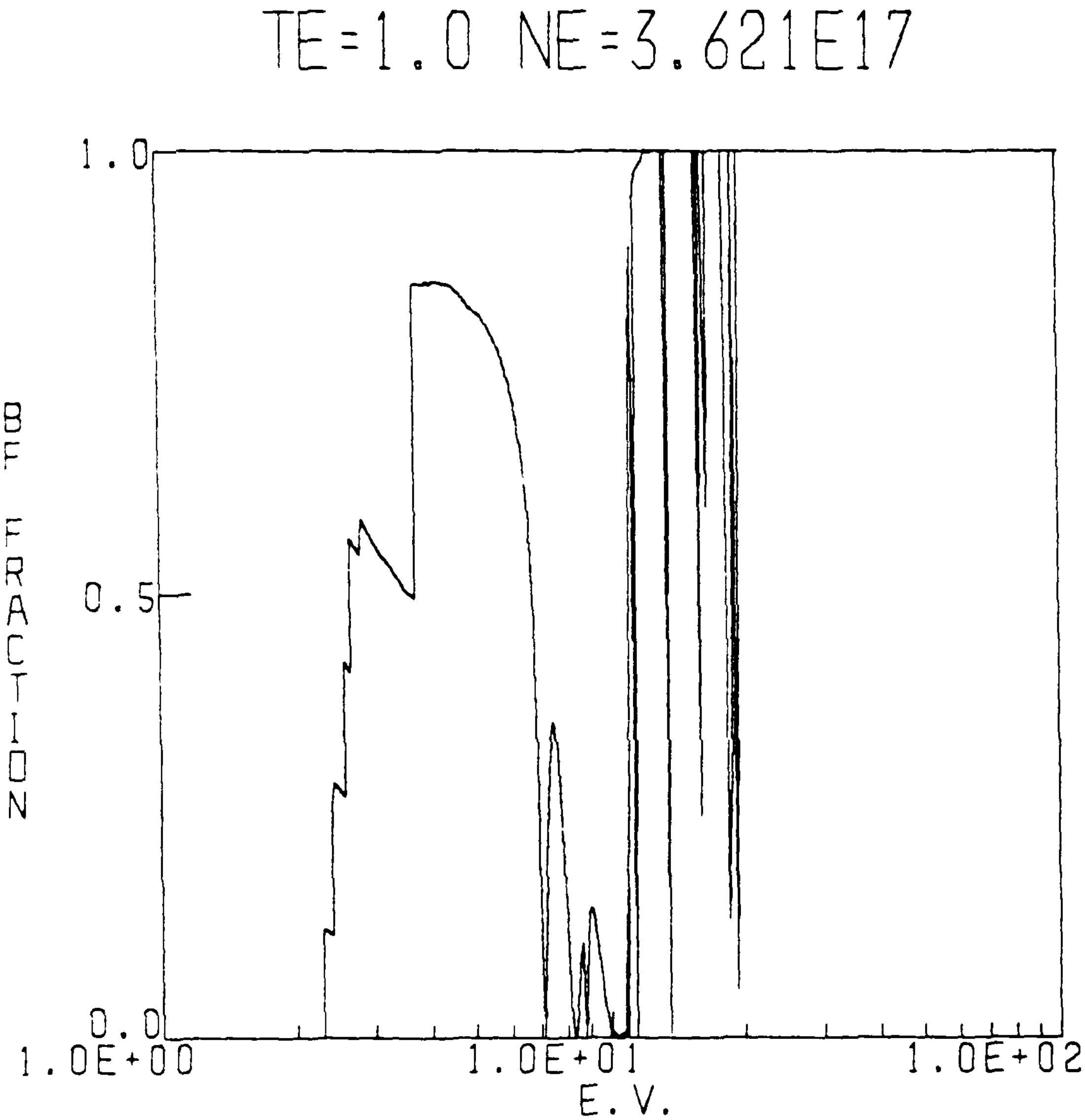

Fig. 1f — Fraction of the total photoabsorption coefficient due to bound-free transitions. Te = 1.0 e.v.

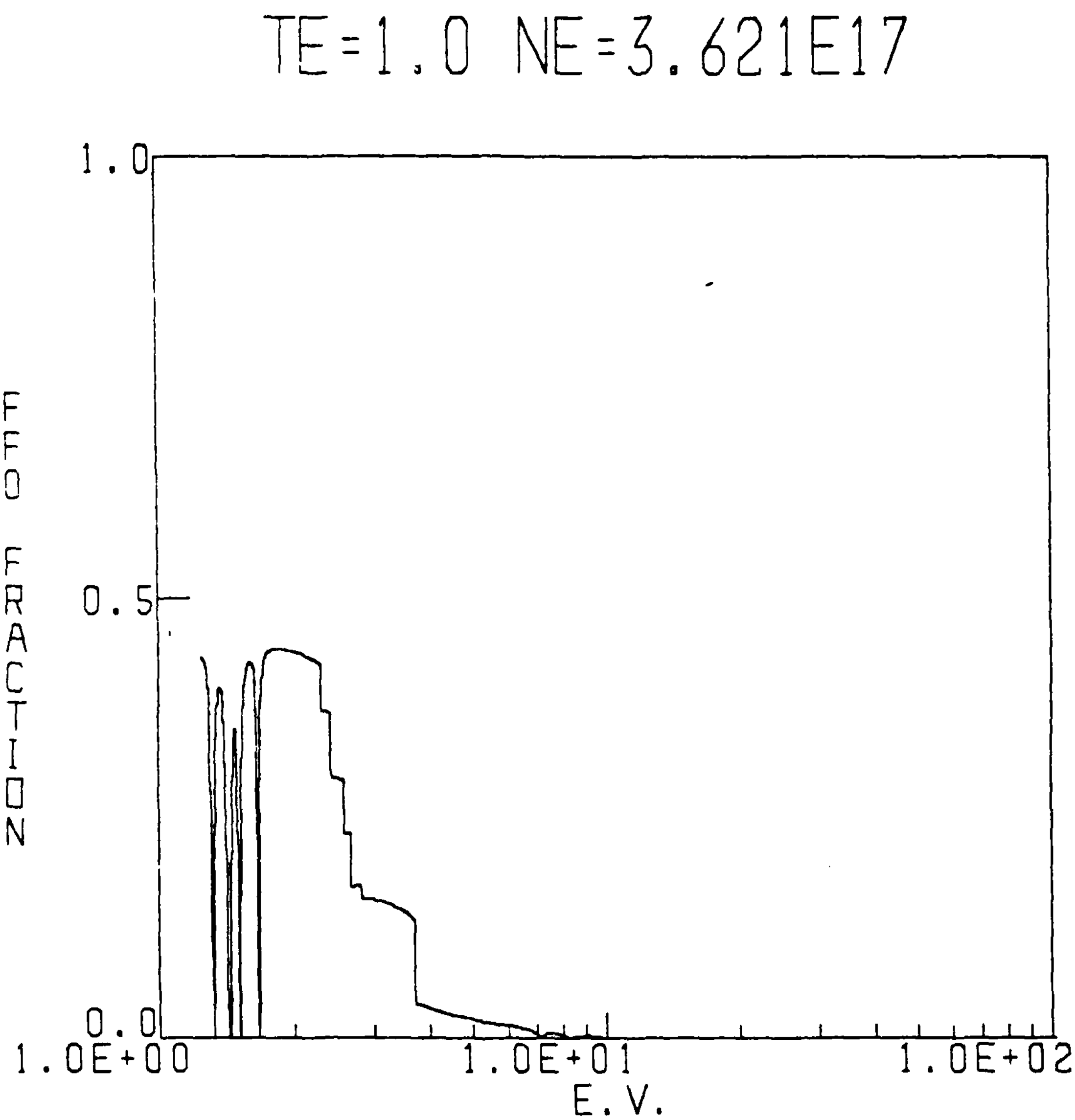

Fig. 1g — Fraction of the total photoabsorption coefficient due to free-free transitions involving neutrals. Te = 1.0 e.v.

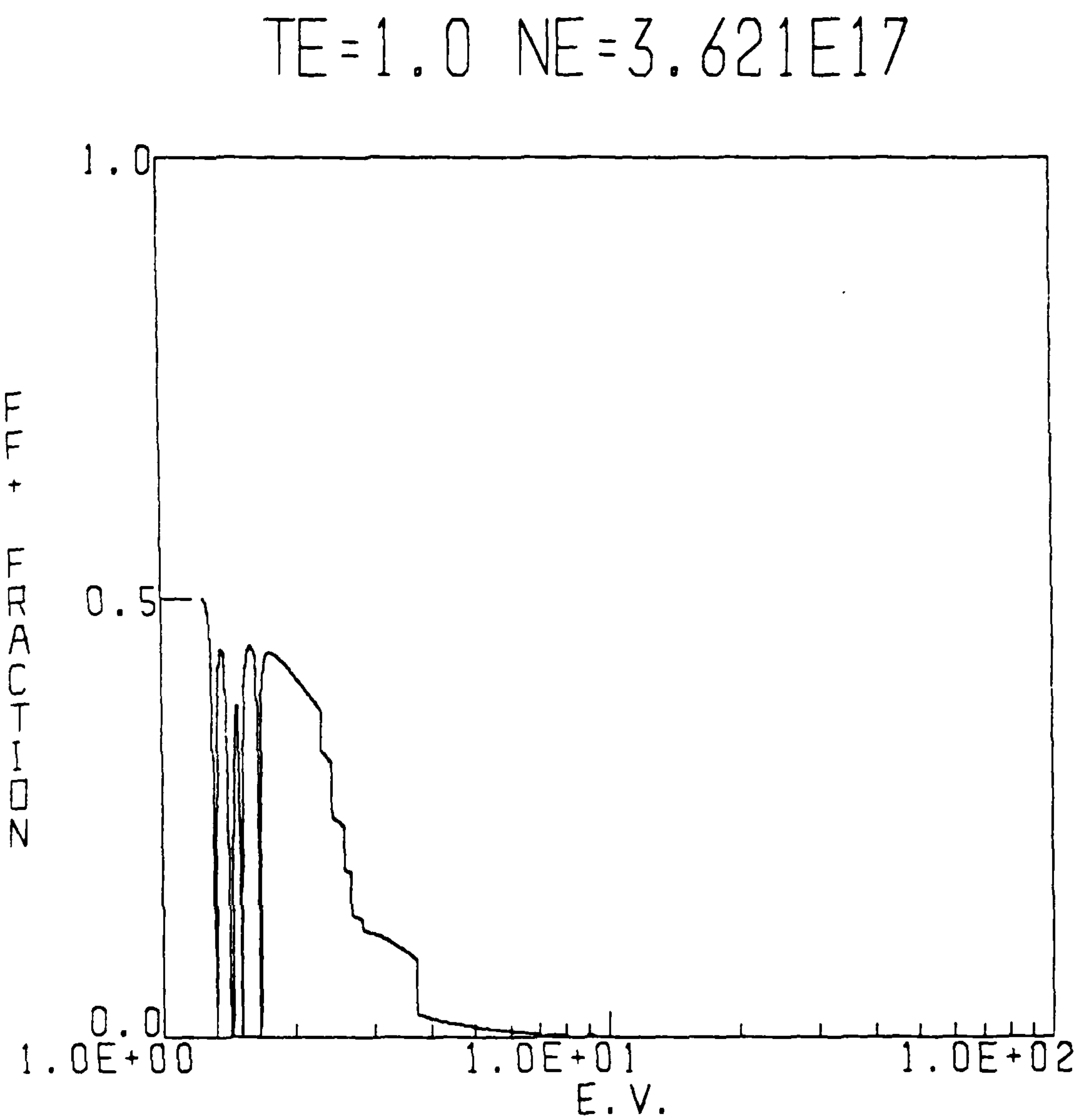

Fig. 1h — Fraction of the total photoabsorption coefficient due to free-free transitions involving ions. Te = 1.0 e.v.

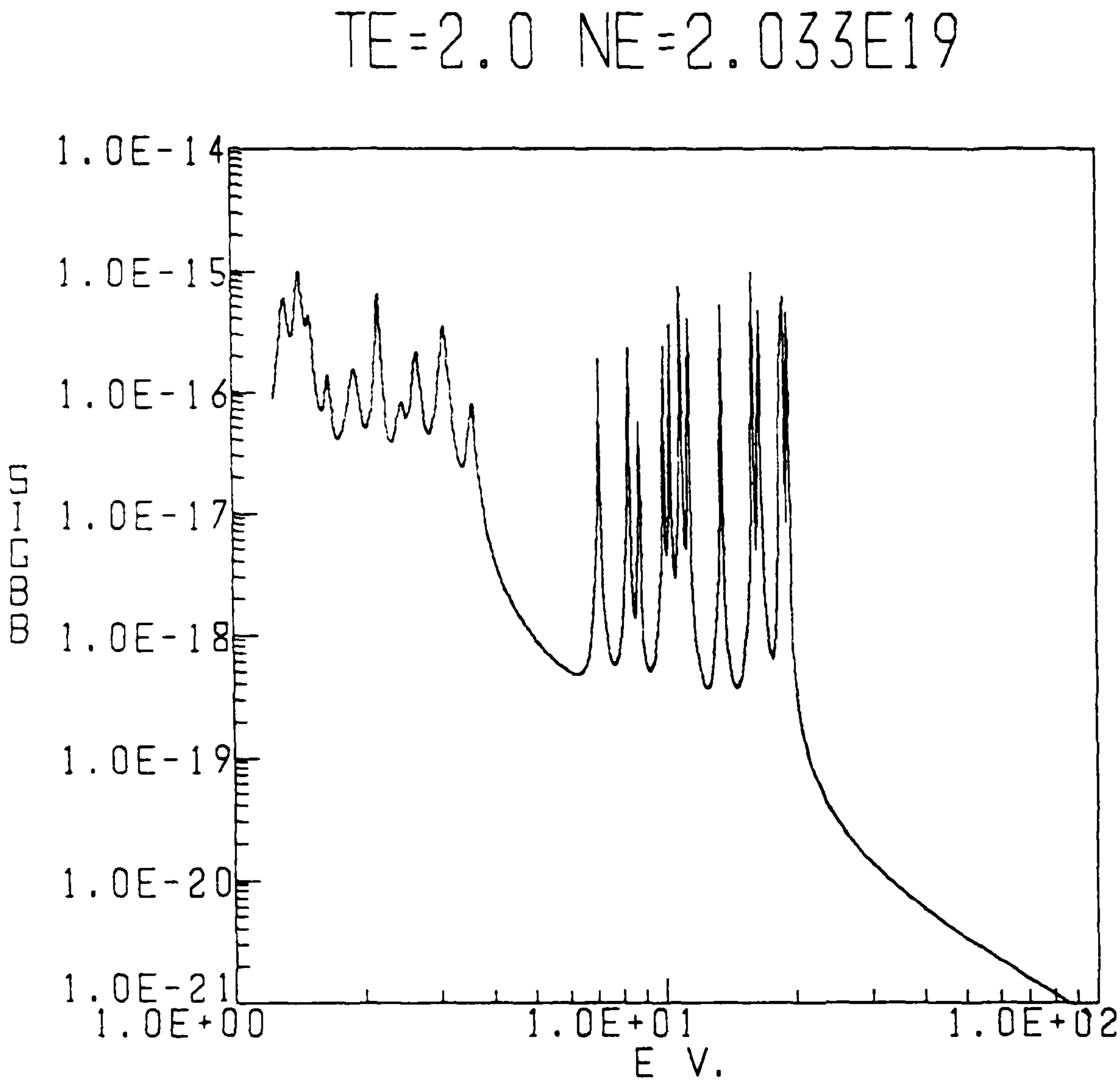

Fig. 2a — Same as Figure 1a. Te = 2.0 e.v.

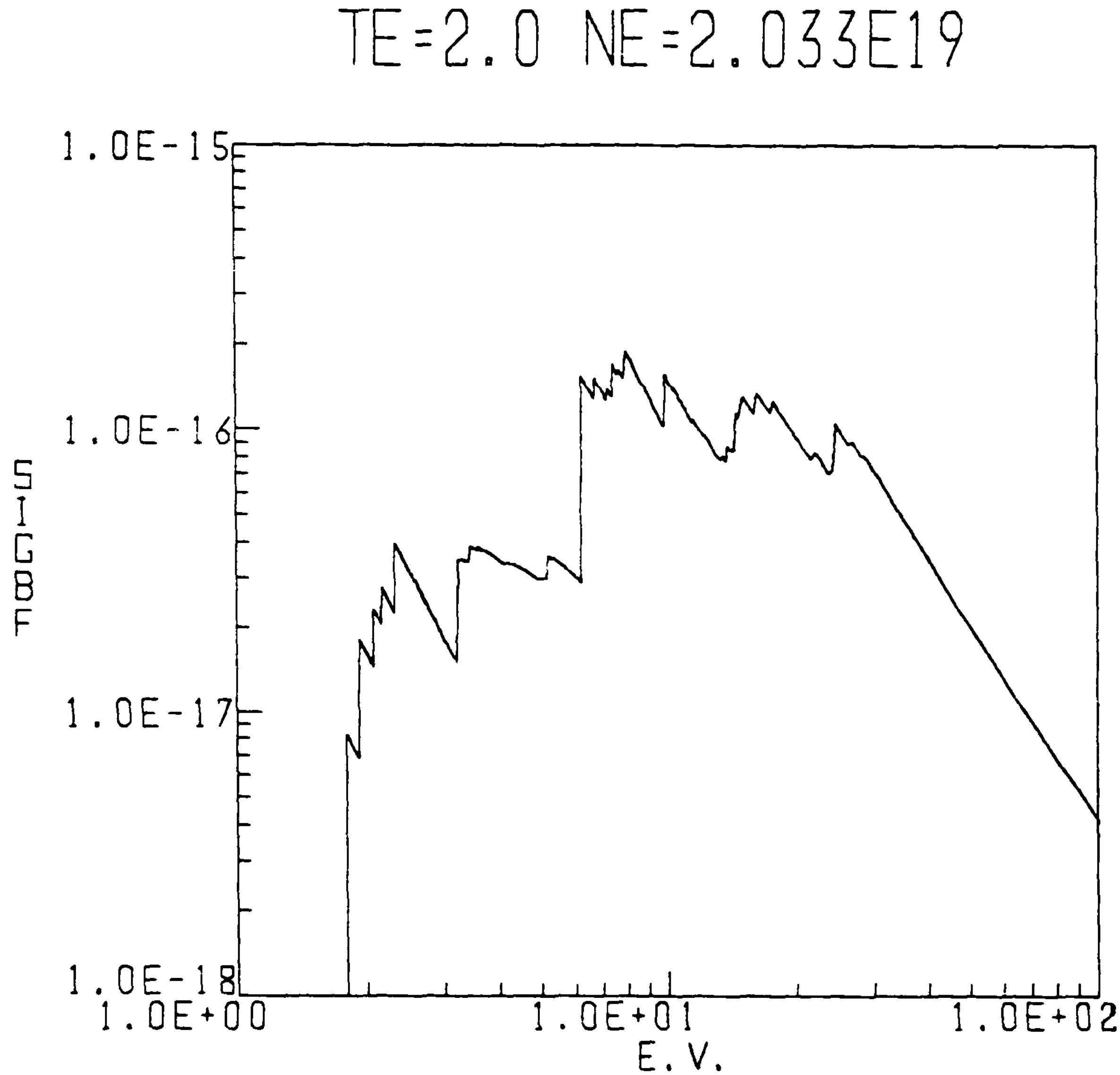

Fig. 2b — Same as Figure 1b. Te = 2.0 e.v.

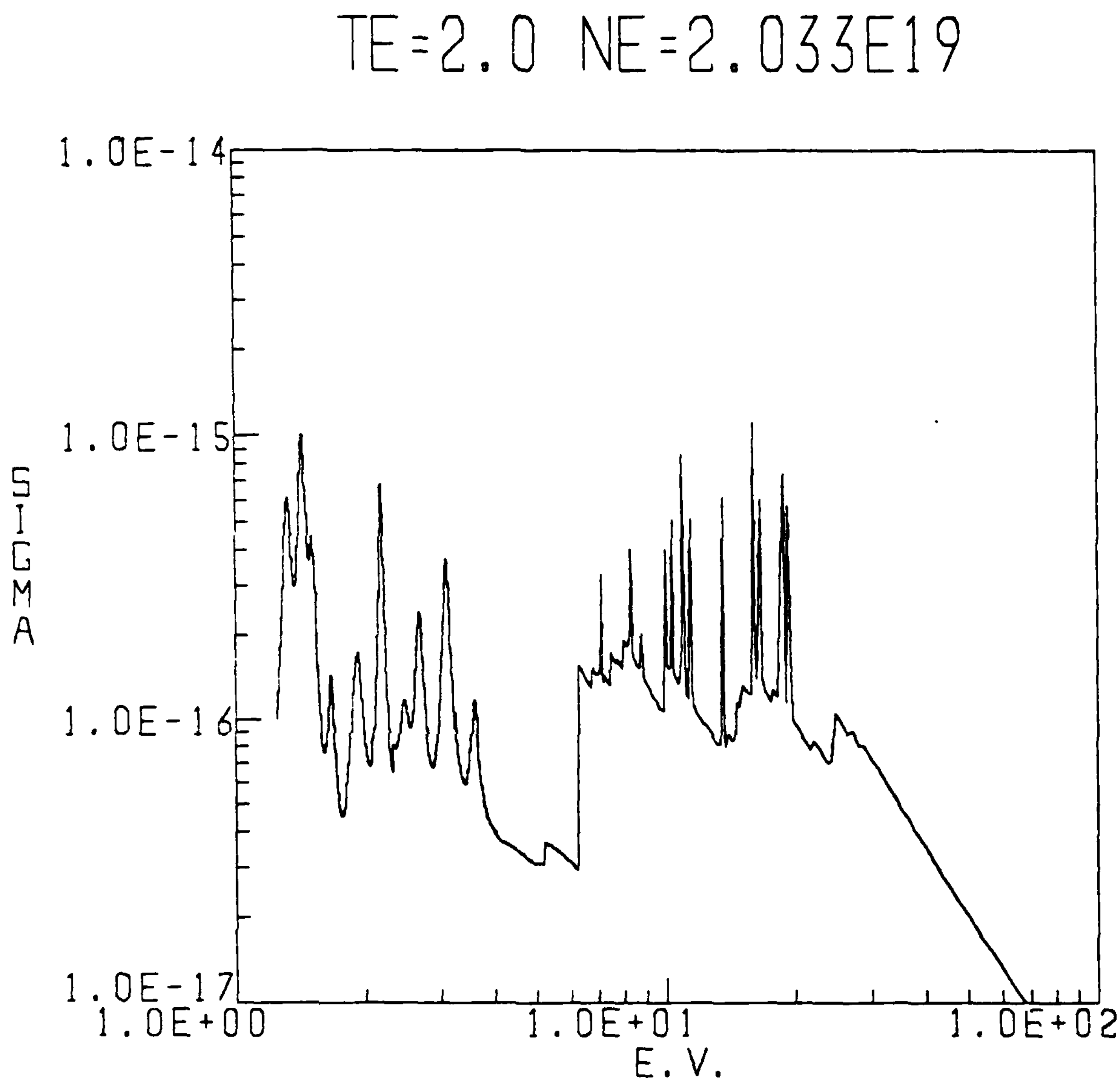

Fig. 2c — Same as Figure 1c. Te = 2.0 e.v.

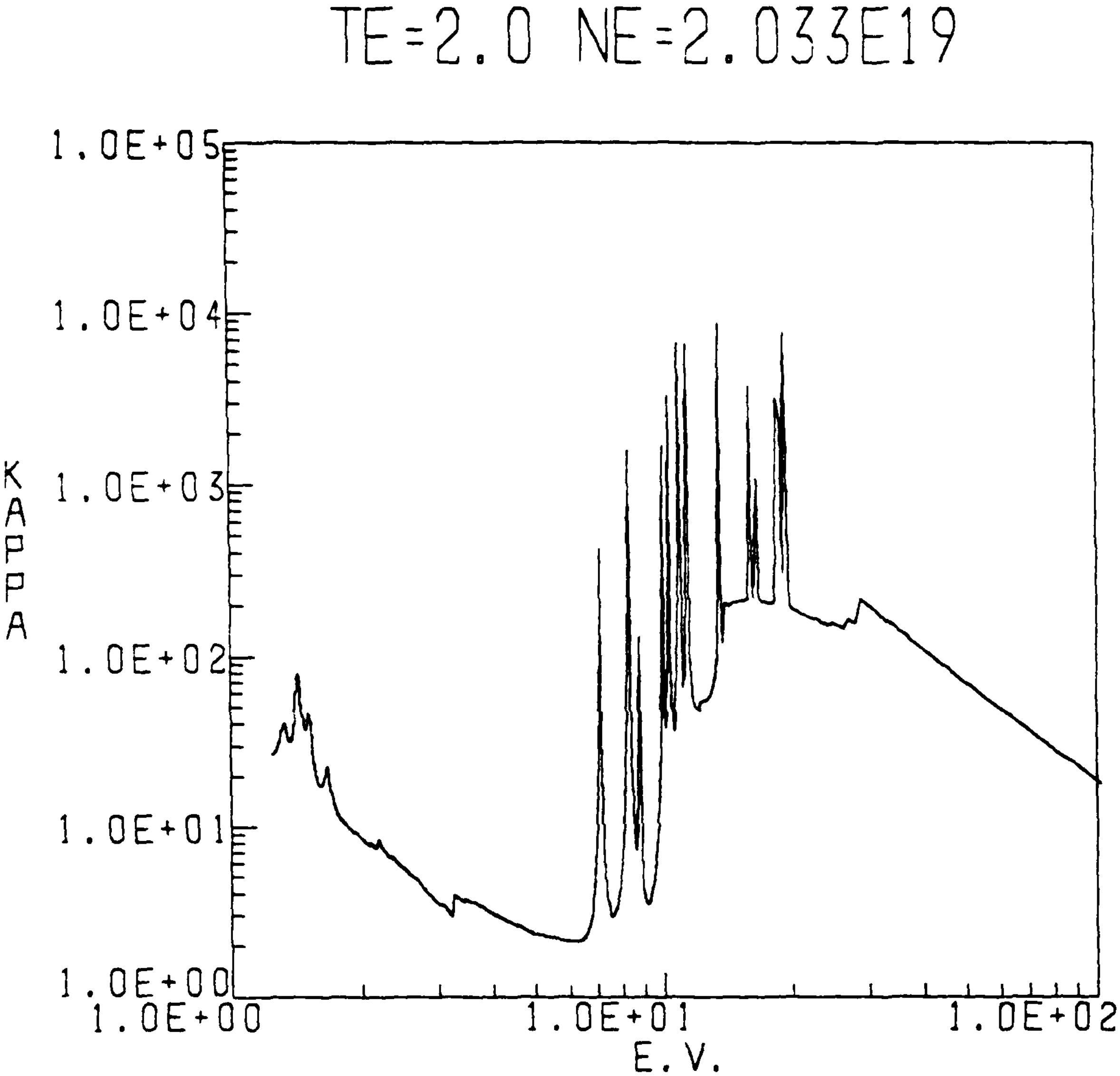

Fig. 2d — Same as Figure 1d. Te = 2.0 e.v.

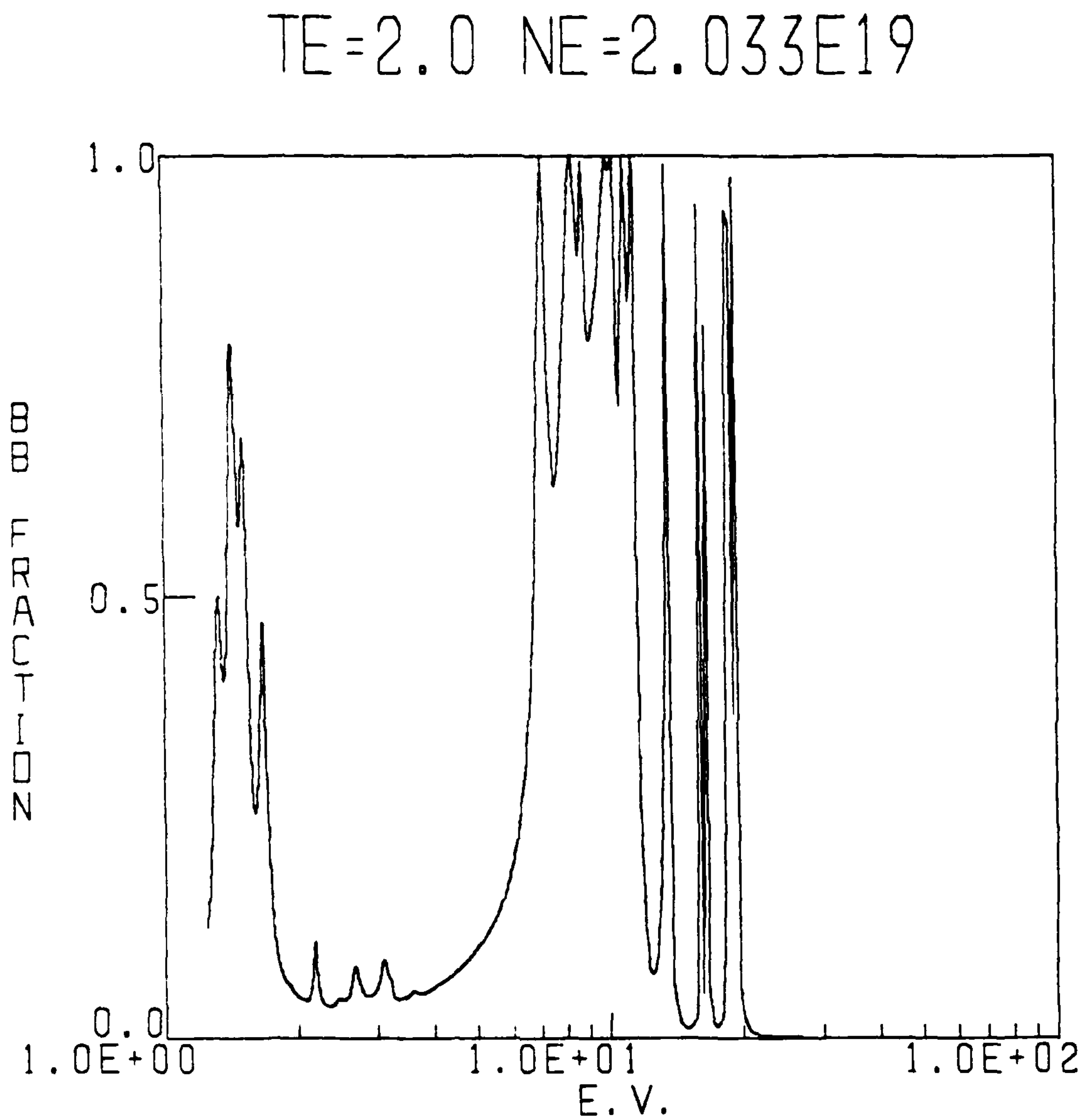

Fig. 2e — Same as Figure 1e. Te = 2.0 e.v.

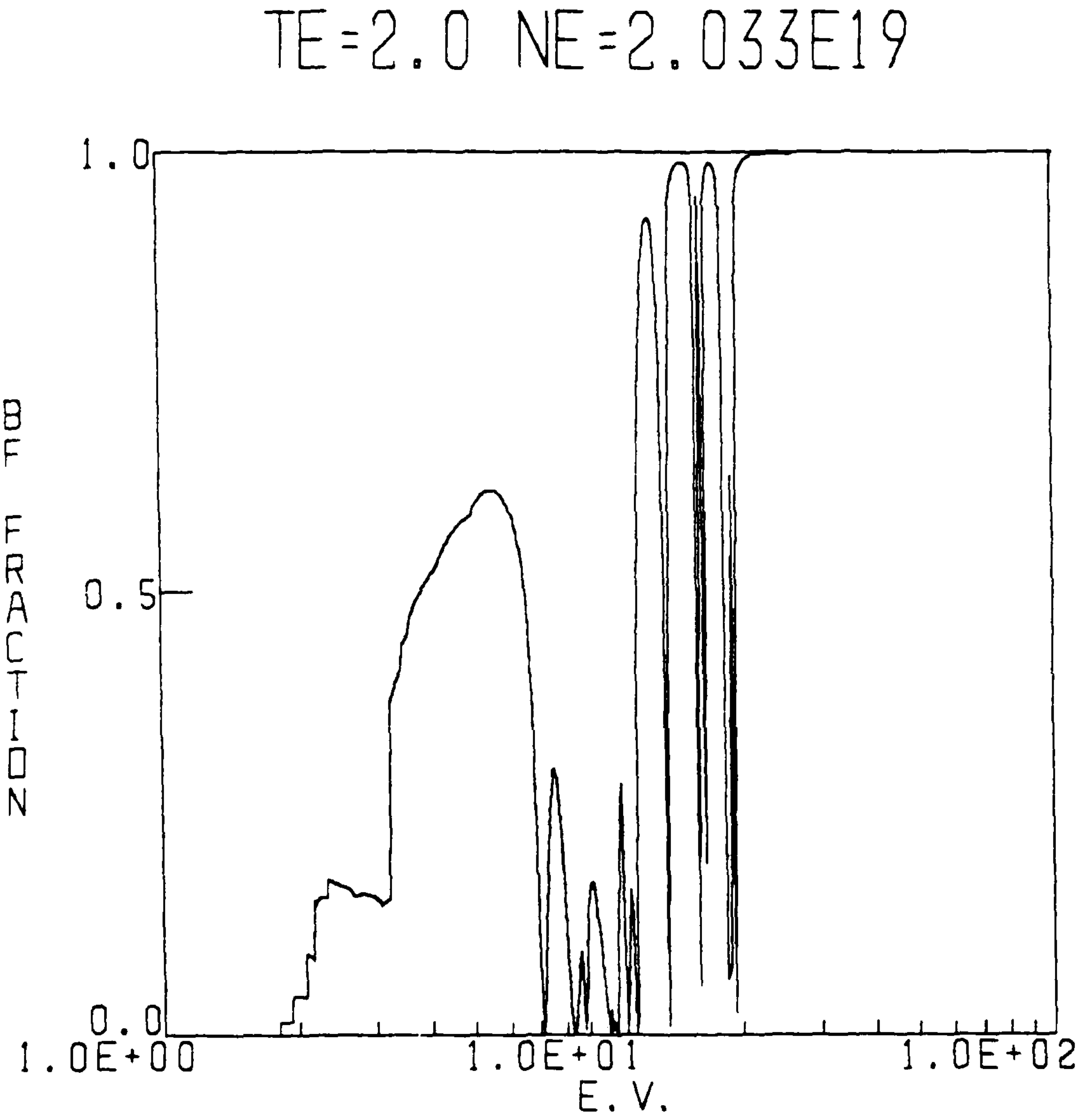

Fig. 2f — Same as Figure 1f. Te = 2.0 e.v.

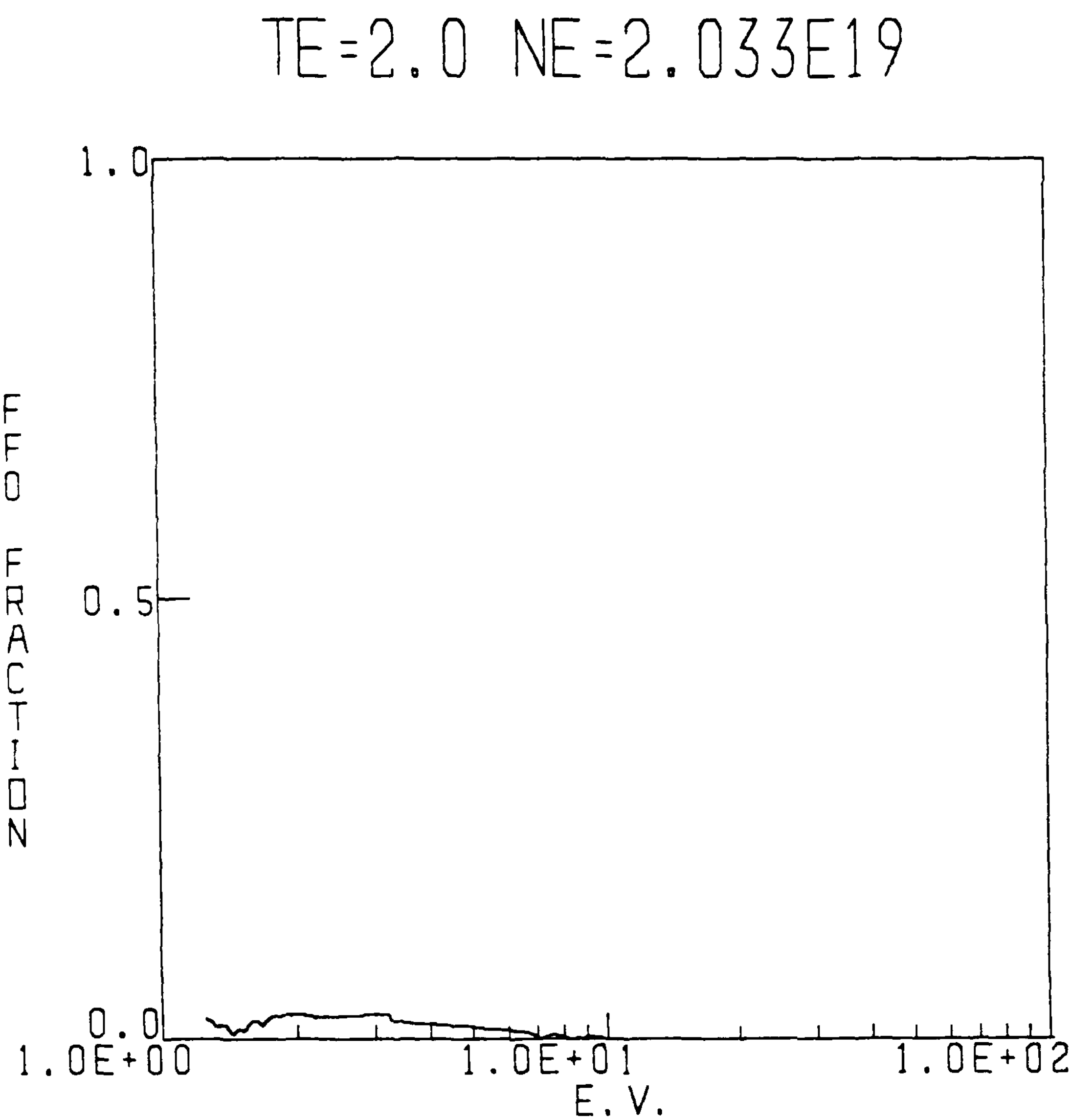

Fig. 2g — Same as Figure 1g. Te = 2.0 e.v.

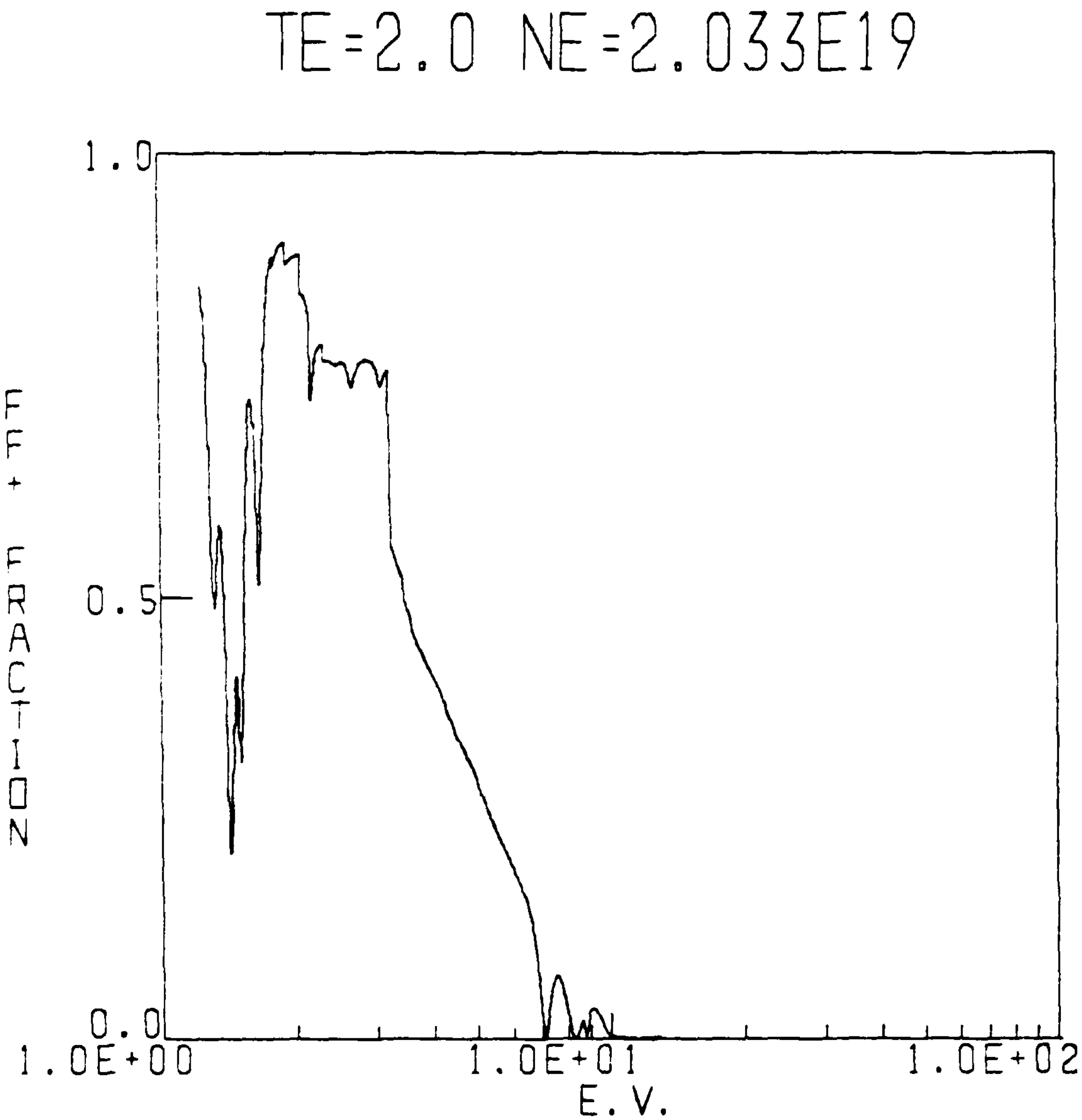

Fig. 2h — Same as Figure 1h. Te = 2.0 e.v.

TE=3.0 NE=3.677E19

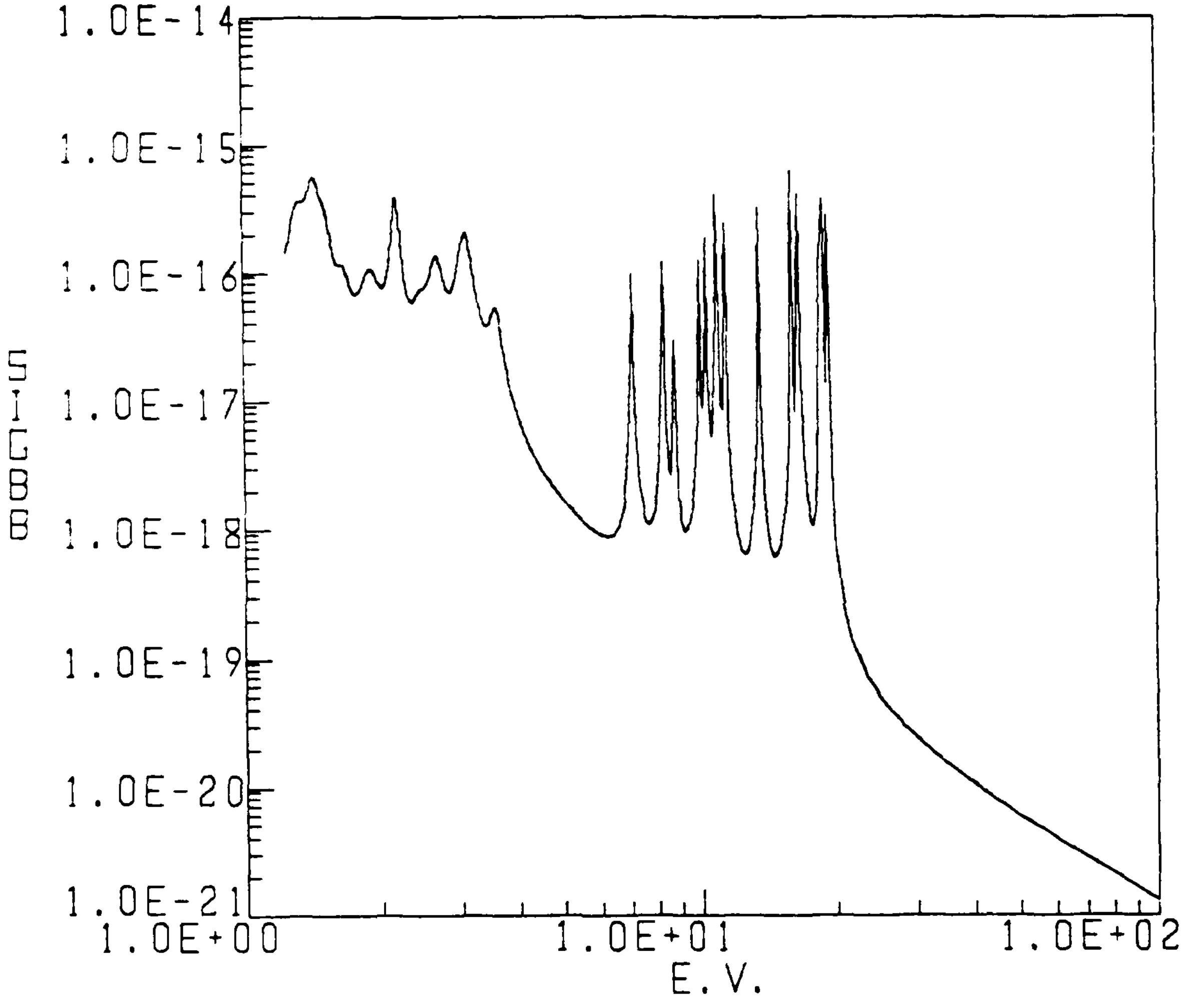

Fig. 3a — Same as Figure 1a. Te = 3.0 e.v.

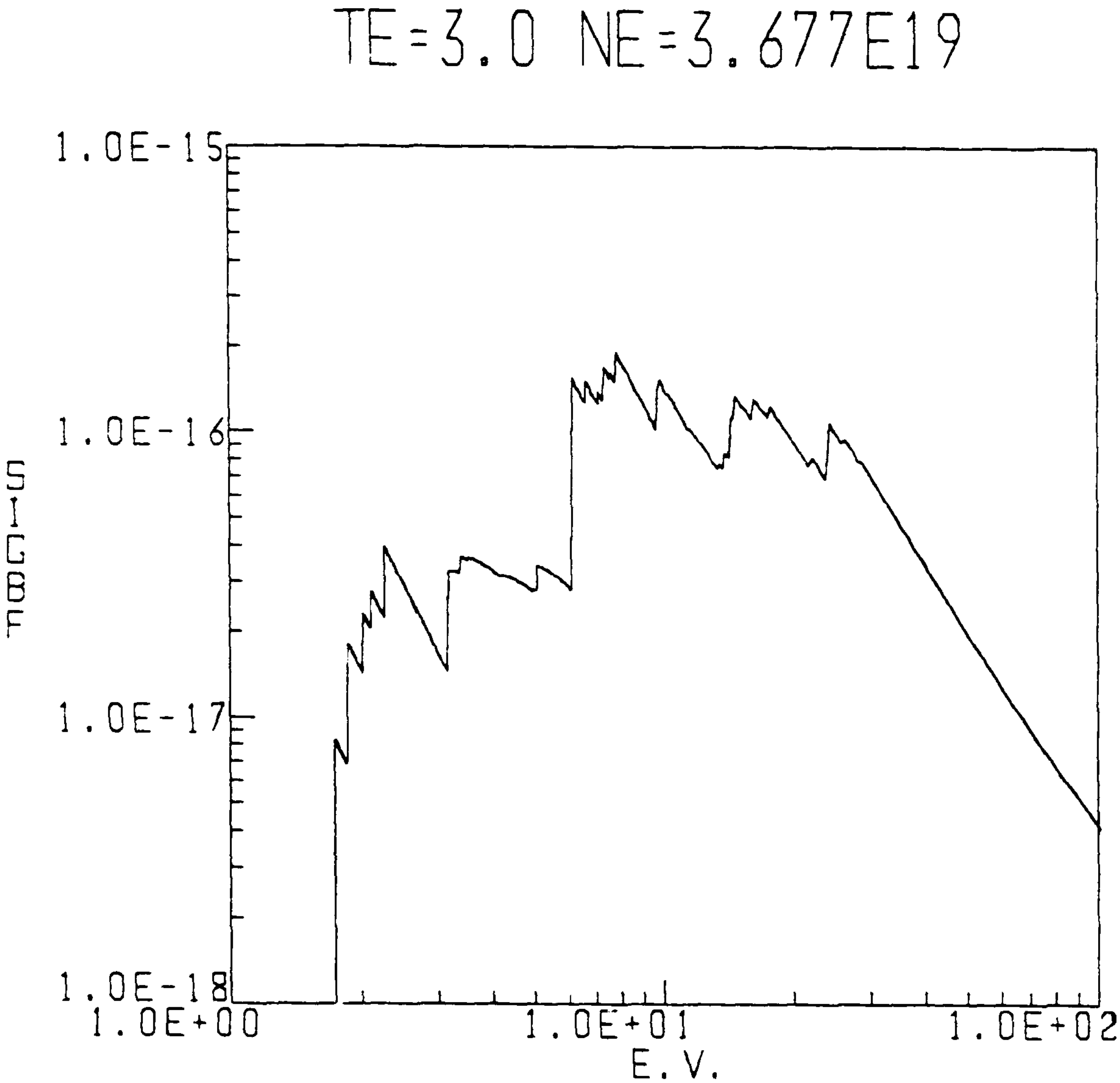

Fig. 3b — Same as Figure 1b. Te = 3.0 e.v.

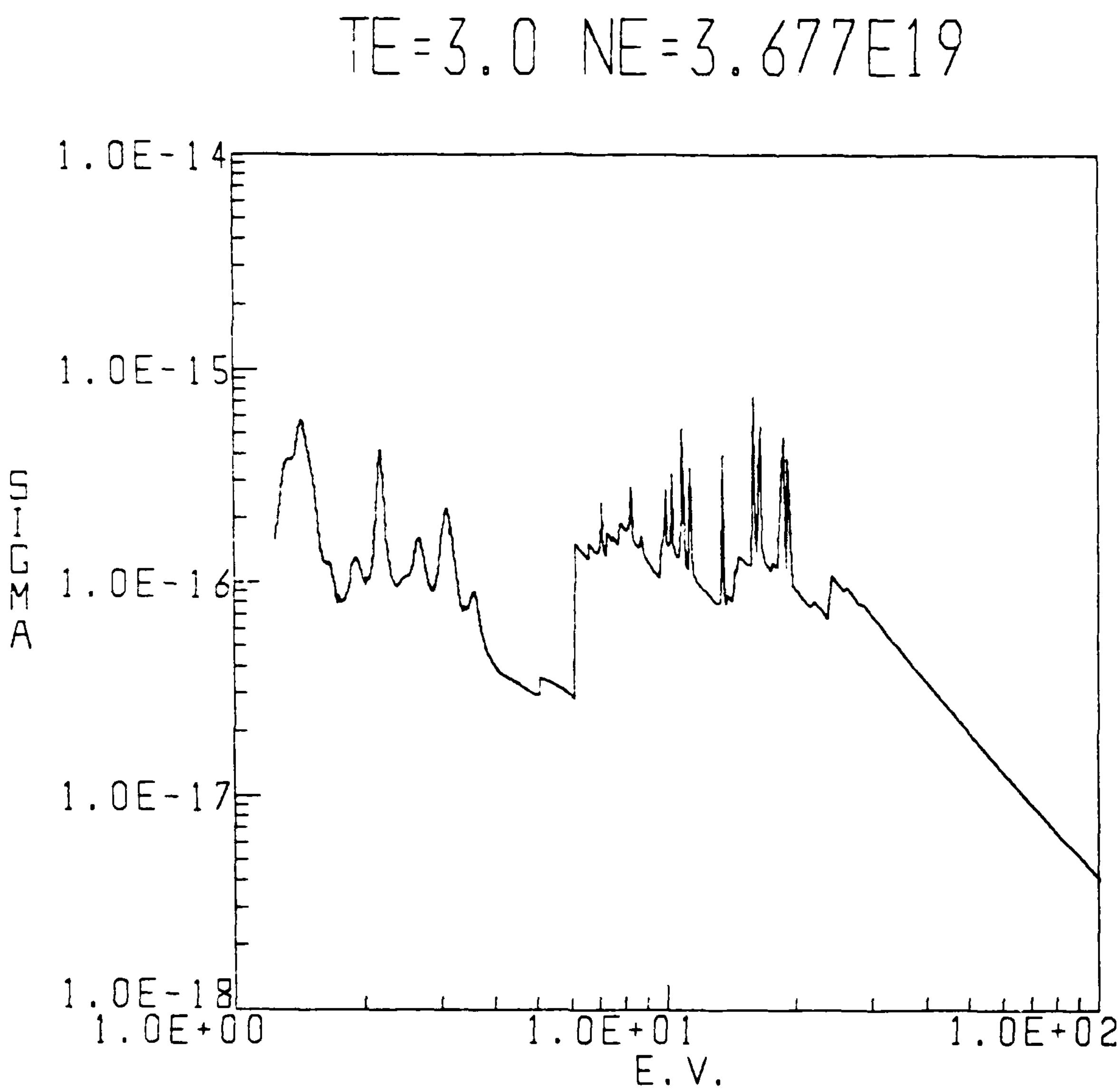

Fig. 3c — Same as Figure 1c. Te = 3.0 e.v.

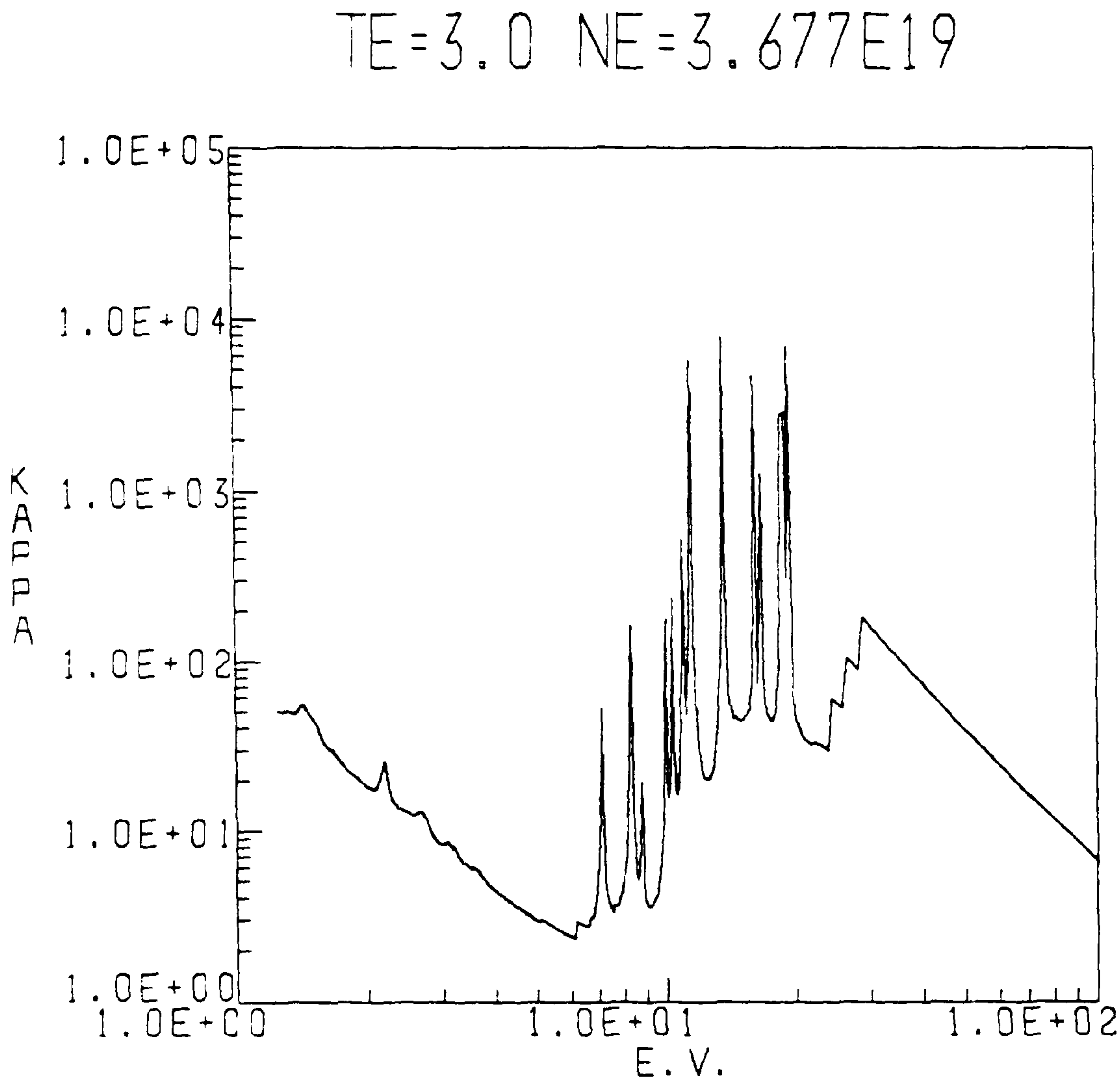

Fig. 3d — Same as Figure 1d. Te = 3.0 e.v.

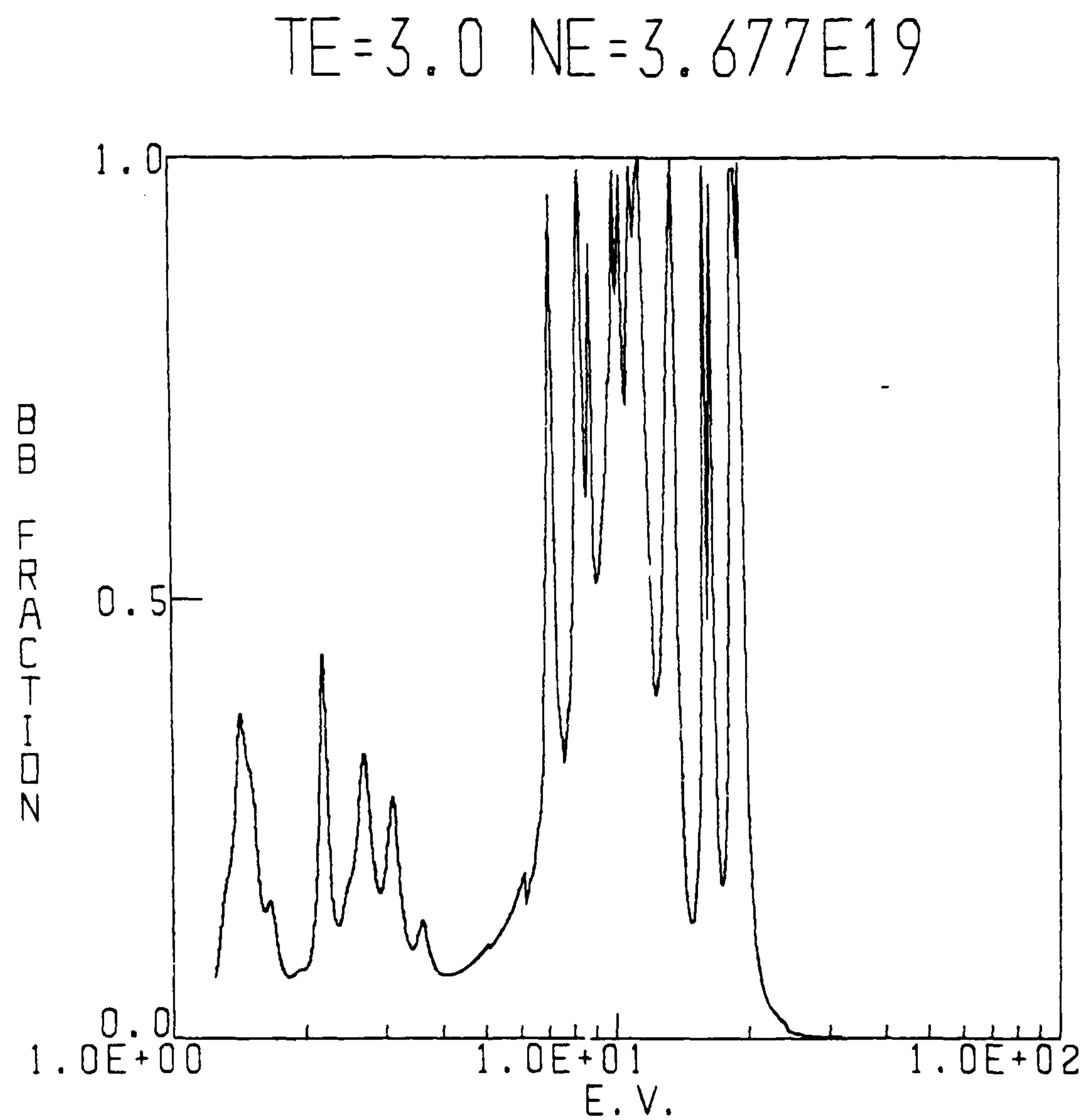

Fig. 3e — Same as Figure 1e. Te = 3.0 e.v.

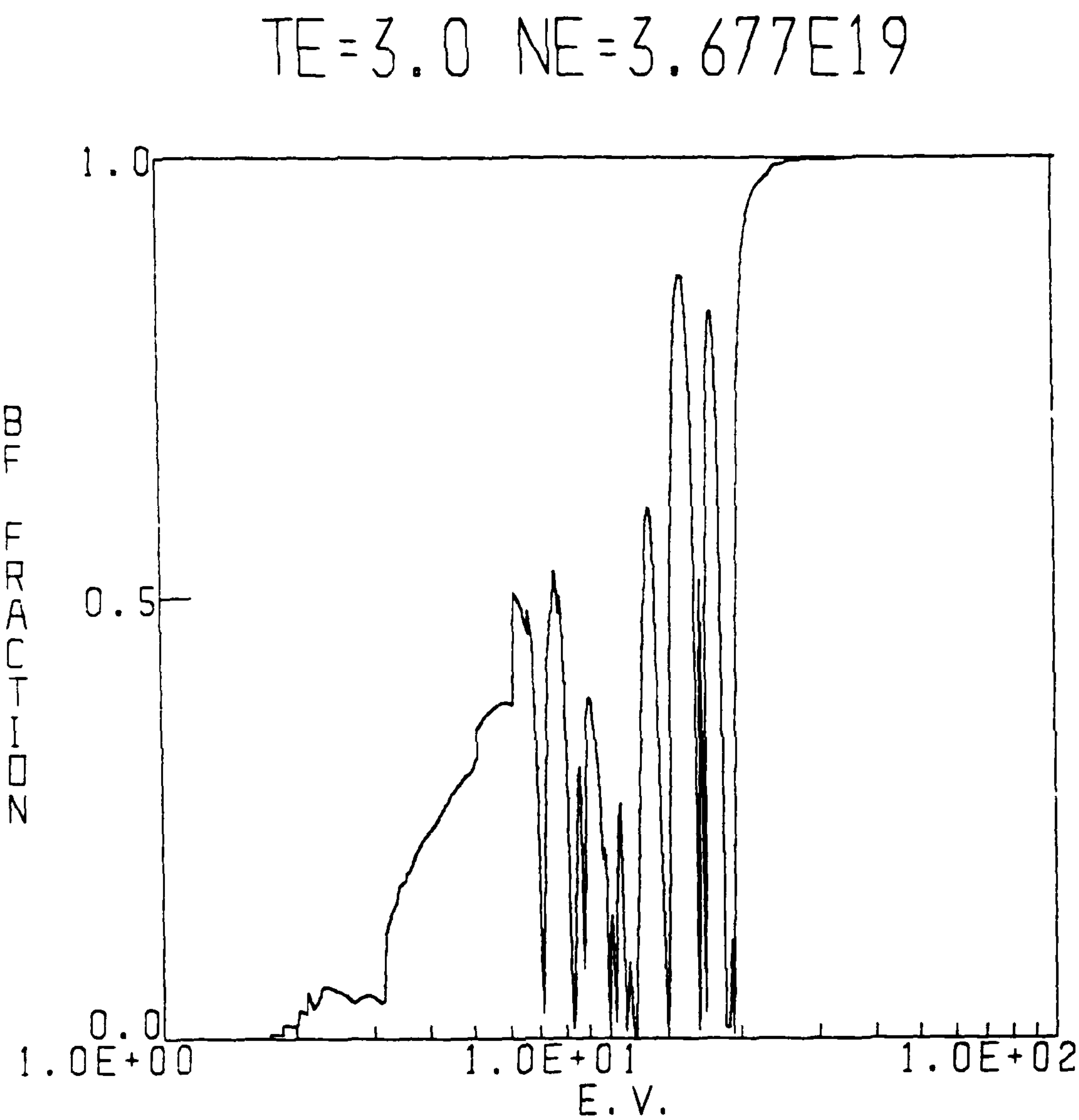

Fig. 3f — Same as Figure 1f. Te = 3.0 e.v.

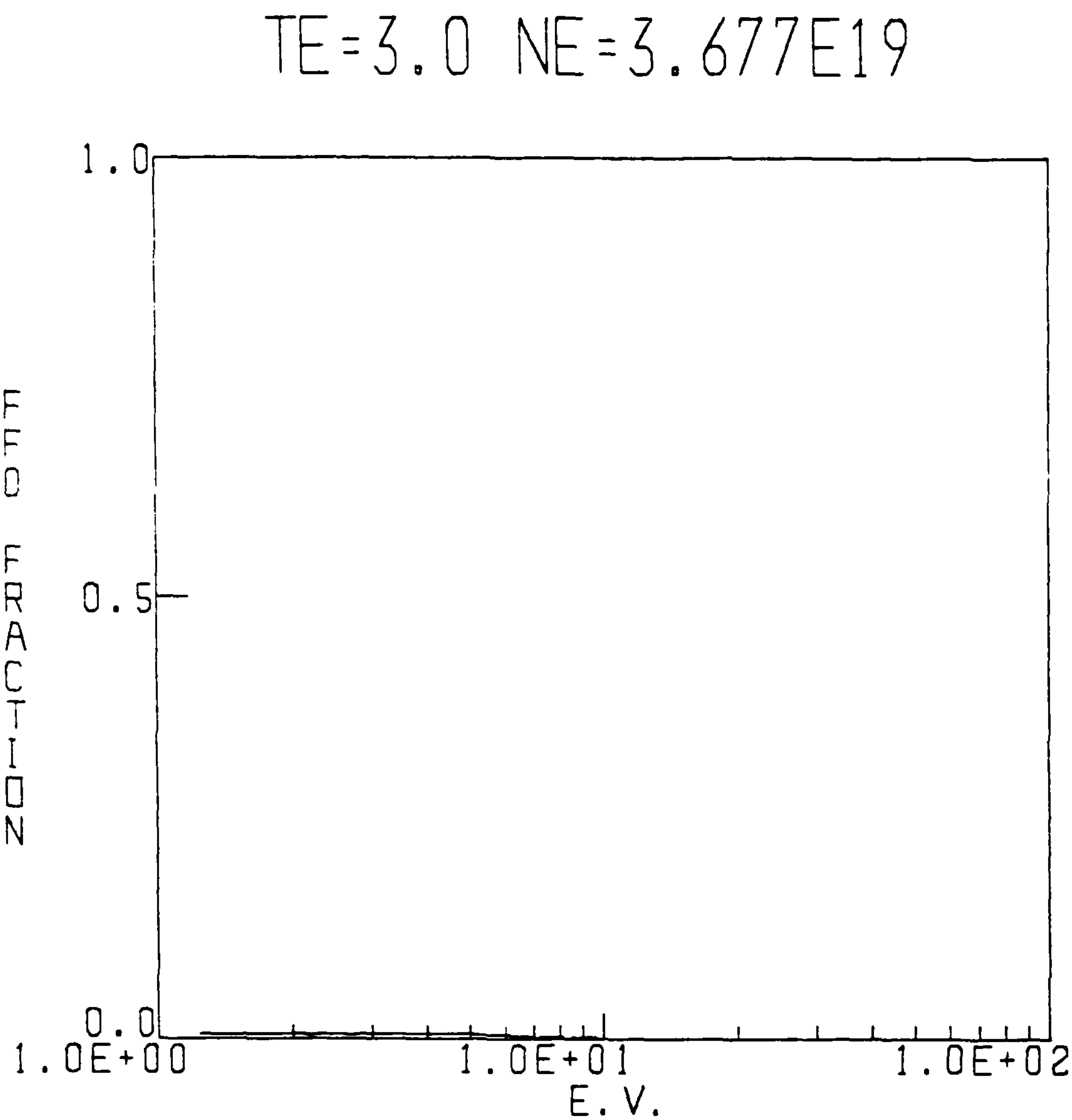

Fig. 3g — Same as Figure 1g. Te = 3.0 e.v.

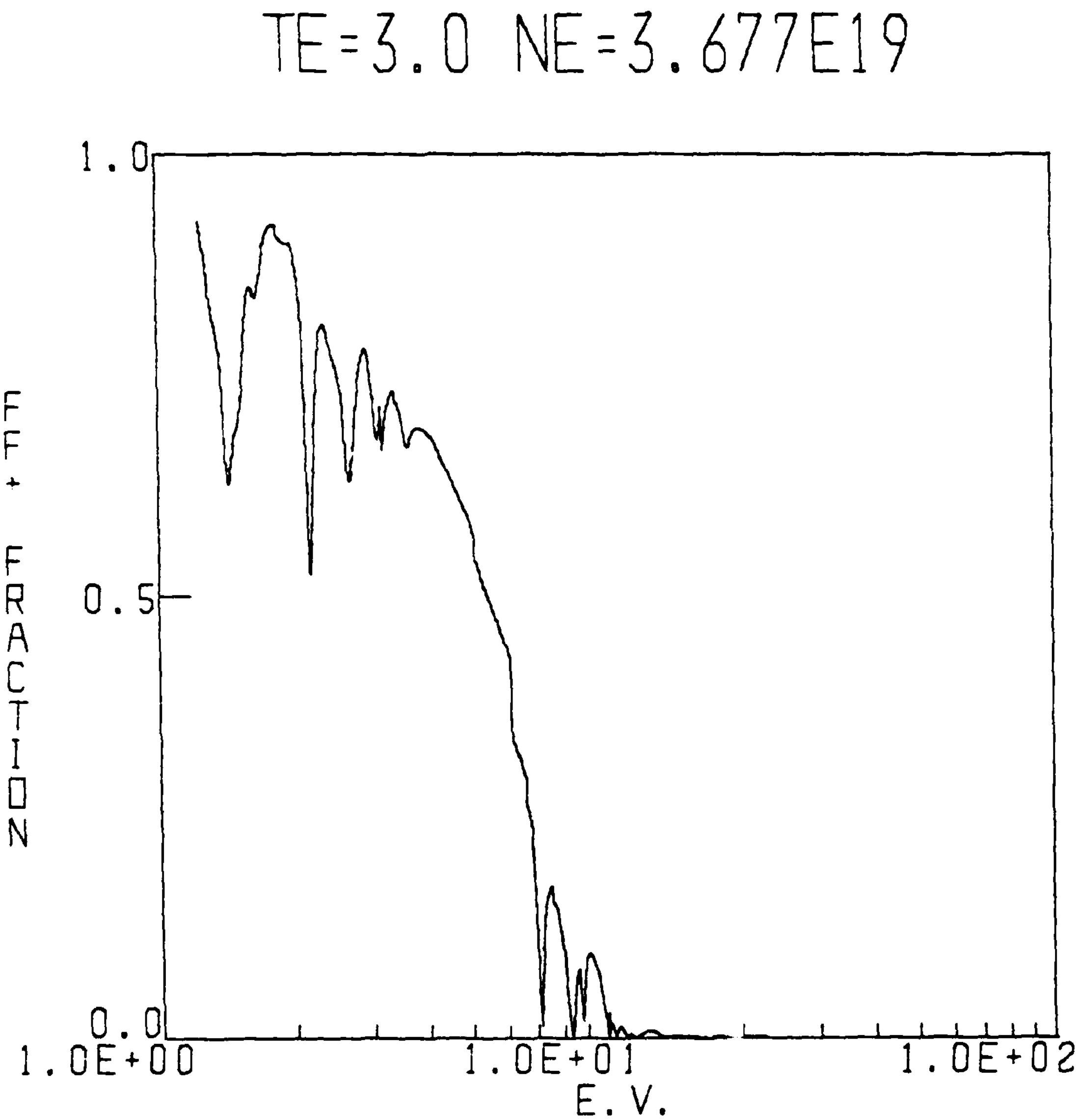

Fig. 3h — Same as Figure 1h. Te = 3.0 e.v.

REFERENCES

1. R.D.Taylor and A.W. Ali, "Recombination and Ionization in a Nitrogen Plasma", NRL Memorandum Report (in press).

2. Y.B. Zeldovich and Y.P. Raiser, Physics of Shock Waves and High-Temperature Hydrodynamic Phenomena, Academic Press, New York (1966).

3. a. R.R. Johnston, R.K.M. Landshoff, and O.R. Platas, "Radiative Properties of High Temperature Air", Lockheed Report LMSC D267205 (1972).

   b. R.R. Johnston and D.E. Stevenson, "Radiative Properties of High Temperature Air, II", SAI Report (1977).

4. H.R. Griem, Spectral Line Broadening by Plasmas, Academic Press, New York (1974).

5. R.J.W. Henry, Astrophys. J. 161, 1153 (1970).

6. a. A.W. Ali, "Photoionization Cross Sections of O and N Atoms and Their Low Lying Metastable States", NRL Plasma Dynamics Technical Note 32 (1971).

   b. A.W. Ali, "The Physics of the Photodeposition Phase of the NRL Master Code for the Disturbed E and F Regions", NRL Memorandum Report 4152 (1980). (AD-A081 776)

7. H.R. Griem, Plasma Spectroscopy, McGraw-Hill Book Co., New York (1964).

8. See, for example, J.W. Bond, K.M. Watson, and J.A. Welch, Atomic Theory of Gas Dynamics, Addison-Wesley, Reading, Mass. (1965) and references therein.

9. R. C. Mjolsness and H. M. Ruppel, J.Q.S.R.T., 7, 423 (1967).

10. S. Geltman, J.Q.S.R.T., 13, 601 (1973).

11. F.R. Gilmore, "Equilibrium Composition and Thermodynamic Properties of Air to 24000 °K", RAND Report RM-1543 (1955). (AD-084052)

DISTRIBUTION LIST

Chief of Naval Operations
Washington, DC 20350
ATTN: Dr. C. F. Sharn (OP0987B)

U. S. Army Ballistics Research Laboratory
Aberdeen Proving Ground, Maryland 21005
ATTN: Dr. Donald Eccleshall (DRXBR-BM)
Dr. Anand Prakash

Office of Under Secretary of Defense
Research and Engineering
Room 3E1034
The Pentagon
Washington, DC 20301
ATTN: Mr. John M. Bachkosky

Office of Naval Research
800 North Quincy Street
Arlington, VA 22217
ATTN: Dr. C. W. Roberson

Chief of Naval Material
Office of Naval Technology
MAT-0712, Room 503
800 North Quincy Street
Arlington, VA 22217
ATTN: Dr. Eli Zimet

Commander
Naval Sea Systems Command
PMS-405
Washington, DC 20362
ATTN: CAPT R. Topping
CDR W. Bassett

Air Force Office of Scientific Research
Physical and Geophysical Sciences
Bolling Air Froce Base
Washington, DC 20332
ATTN: CAPT Henry L. Pugh, Jr.

Department of Energy
Washington, DC 20545
ATTN: Dr. Terry F. Godlove (ER20:GTN, High Energy and Nuclear Physics)
Dr. James E. Leiss (G-256)
Mr. Gerald J. Peters (G-256)

Joint Institute for Laboratory Astrophysics
National Bureau of Standards and
University of Colorado
Boulder, CO 80309
ATTN: Dr. Arthur V. Phelps

Lawrence Berkeley Laboratory
University of California
Berkeley, CA 94720
ATTN: Dr. Edward P. Lee

Ballistic Missile Defense Advanced Technology Center
P.O. Box 1500
Huntsville, AL 35807
ATTN: Dr. M. Hawie (BMDSATC-1)

Intelcom Rad Tech.
P.O. Box 81087
San Diego, CA 92138
ATTN: Dr. W. Selph

Lawrence Livermore National Laboratory
University of California
Livermore, CA 94550
ATTN: Dr. Richard J. Briggs
Dr. Thomas Fessenden
Dr. Frank Chambers
Dr. James W.-K. Mark, L-477
Dr. William Fawley
Dr. William Barletta
Dr. William Sharp
Dr. Daniel S. Prono
Dr. John K. Boyd
Dr. Kenneth W. Struve
Dr. John Clark
Dr. George J. Caporaso
Dr. William E. Martin
Dr. Donald Prosnitz
Dr. S. Yu

Mission Research Corporation
735 State Street
Santa Barbara, CA 93102
ATTN: Dr. C. Longmire
Dr. N. Carron

National Bureau of Standards
Gaithersburg, MD 20760
ATTN: Dr. Mark Wilson

Science Applications, Inc.
1200 Prospect Street
La Jolla, CA 92037
ATTN: Dr. M. P. Fricke
Dr. W. A. Woolson

Science Applications, Inc.
5 Palo Alto Square, Suite 200
Palo Alto, CA 94304
ATTN: Dr. R. R. Johnston
Dr. Leon Feinstein
Dr. Douglas Keeley

Science Applications, Inc.
1651 Old Meadow Road
McLean, VA 22101
ATTN: Mr. W. Chadsey

Naval Surface Weapons Center
White Oak Laboratory
Silver Spring, MD 20910
ATTN: Mr. R. J. Biegalski
Dr. R. Cawley
Dr. J. W. Forbes
Dr. D. L. Love
Dr. C. M. Huddleston
Dr. G. E. Hudson
Mr. W. M. Hinckley
Mr. N. E. Scofield
Dr. E. C. Whitman
Dr. M. H. Cha
Dr. H. S. Uhm
Dr. R. Fiorito
Dr. H. C. Chen

C. S. Draper Laboratories
Cambridge, MA 02139
ATTN: Dr. E. Olsson
Dr. L. Matson

Physcal Dynamics, Inc.
P.O. Box 1883
La Jolla, CA 92038
ATTN: Dr. K. Brueckner

Avco Everett Research Laboratory
2385 Revere Beach Pkwy
Everett, MA 02149
ATTN: Dr. R. Patrick
Dr. Dennis Reilly
Dr. D. H. Douglas-Hamilton

Defense Technical Information Center
Cameron Station
5010 Duke Street
Alexandria, VA 22314 (2 copies)

Naval Research Laboratory
Washington, DC 20375
ATTN: M. Lampe - Code 4792
M. Friedman - Code 4700.1
J. R. Greig - Code 4763
I. M. Vitkovitsky - Code 4701
J. B. Aviles - Code 6650
M. Haftel - Code 6651
T. Coffey - Code 1001
S. Ossakow - Code 4700 (26 copies)
P. Sprangle - Code 4790
Library - Code 2628 (20 copies)
A. W. Ali - Code 4700.1 (30 copies)
D. Book - Code 4040
J. Boris - Code 4040
R. Hubbard - Code 4790
B. Hui - Code 4790
S. Slinker - Code 4790
G. Joyce - Code 4790
D. Murphy - Code 4763
A. Robson - Code 4760
D. Colombant - Code 4790
M. Picone - Code 4040
M. Raleigh - Code 4763
R. Pechacek - Code 4763
G. Cooperstein - Code 4770
Y. Lau - Code 4790
R. Fernsler - Code 4790

Defense Advanced Research Projects Agency
1400 Wilson Blvd.
Arlington, VA 22209
ATTN: Dr. S. Shey

Physics International, Inc.
2700 Merced Street
San Leanadro, CA 94577
ATTN: Dr. E. Goldman

SDIO - DEW
Office of Secretary of Defense
Washington, DC 20301
ATTN: Lt. Col. R. L. Gullickson

Mission Research Corp.
1720 Randolph Road, S.E.
Albuquerque, NM 87106
ATTN: Dr. Brendan Godfrey
Dr. Richard Adler
Dr. Thomas Hughes
Dr. Lawrence Wright

Princeton University
Plasma Physics Laboratory
Princeton, NJ 08540
ATTN: Dr. Francis Perkins, Jr.

McDonnell Douglas Research Laboratories
Dept. 223, Bldg. 33, Level 45
Box 516
St. Louis, MO 63166
ATTN: Dr. Evan Rose
Dr. Carl Leader

Cornell University
Ithaca, NY 14853
ATTN: Prof. David Hammer

Sandia National Laboratory
Albuquerque, NM 87115
ATTN: Dr. Bruce Miller
Dr. Barbara Epstein
Dr. John Freeman
Dr. John E. Brandenburg
Dr. Gordon T. Leifeste
Dr. Carl A. Ekdahl, Jr.
Dr. Gerald N. Hays
Dr. James Chang
Dr. Michael G. Mazerakis

University of California
Physics Department
Irvine, CA 92664
ATTN: Dr. Gregory Benford

Air Force Weapons Laboratory
Kirtland Air Force Base
Albuquerque, NM 87117
ATTN: D. Straw (AFWL/NTYP)
C. Clark (AFWL/NTYP)
W. Baker (AFWL/NTYP)
D. Dietz (AFWL/NTYP)
Lt Col J. Head

Pulse Sciences, Inc.
14796 Wicks Blvd.
San Leandro, CA 94577
ATTN: Dr. Sidney Putnam
Dr. John Bayless

Los Alamos National Scientific Laboratory
P.O. Box 1663
Los Alamos, NM 87545
ATTN: Dr. L. Thode
Dr. A. B. Newberger, X-3, MS-608
Dr. M. A. Mostrom, MS-608
Dr. T. P. Starke, MS-942
Dr. H. Dogliani, MS-5000

Institute for Fusion Studies
University of Texas at Austin
RLM 11.218
Austin, TX 78712
ATTN: Prof. Marshall N. Rosenbluth

University of Michigan
Dept. of Nuclear Engineering
Ann Arbor, MI 48109
ATTN: Prof. Terry Kammash
Prof. R. Gilgenbach

Directed Technologies, Inc.
226 Potomac School Road
McLean, VA 22101
ATTN: Dr. Ira F. Kuhn
Dr. Nancy Chesser

Titan Systems, Inc.
8950 Villa La Jolla Drive-Suite 2232
La Jolla, CA 92037
ATTN: Dr. H. L. Buchanon
Dr. R. M. Dowe

Lockheed Palo Alto Laboratory
3251 Hanover Street
Bldg. 203, Dept. 52-11
Palo Alto, CA 94304
ATTN: Dr. John Siambis

University of Maryland
Physics Department
College Park, MD 20742
ATTn: Dr. Y. C. Lee
Dr. C. Grebogi

Science Applications, Inc.
1710 Goodridge Dr.
McLean, VA 22102
ATTN: Dr. A. Drobot
Dr. K. Papadopoulos

Dr. John P. Jackson
Kaman Sciences
1500 Garden of the Gods Road
Colorado Springs, CO 80933

DASIAC - DETIR
Kaman Tempo
25600 Huntington Avenue, Suite 500
Alexandria, VA 22303
ATTN: Mr. F. Wimenitz

Director of Research
U.S. Naval Academy
Annapolis, MD 21402 (2 copies)